BMC Plant Biology

RESEARCH

Open Access

Combined transcriptomic and metabolomic analysis revealed the salt tolerance mechanism of *Populus talassica* × *Populus euphratica*

Ying Liu[1,2], Mengxu Su[1], Xiaoqing Zhao[2,3], Meilin Liu[1], Jiaju Wu[1], Xiaofeng Wu[1], Zhanyuan Lu[2,3*] and Zhanjiang Han[1*]

Abstract

Background To investigate the salt tolerance of *Populus talassica* × *Populus euphratica*, morphological and physiological parameters were measured on the second day after the 15th, 30th and 45th days of NaCl treatment, revealing significant effects of NaCl on growth. To further elucidate the mechanisms underlying salt tolerance, transcriptomic and metabolomic analysis were conducted under different NaCl treatments.

Results The results of morphological and physiological indexes showed that under low salt treatment, *P. talassica* × *P. euphratica* was able to coordinate the growth of aboveground and belowground parts. Under high salt concentration, the growth and water balance of *P. talassica* × *P. euphratica* were markedly inhibited. The most significant differences between treatments were observed on the second day after the 45th day of NaCl treatment.

Transcriptomic analysis showed that the pathways of gene enrichment in the roots and stems of *P. talassica* × *P. euphratica* were different in the salt resistance response. And it involves several core pathways such as plant hormone signal transduction, phenylpropanoid biosynthesis, MAPK signaling pathway—plant, plant- pathogen interaction, carbon metabolism, biosynthesis of amino acids, and several key Transcription factors (TFs) such as AP2/ERF, NAC, WRKY and bZIP.

Metabolomic analysis revealed that KEGG pathway enrichment analysis showed unique metabolic pathways were enriched in *P. talassica* × *P. euphratica* under both 200 mM and 400 mM NaCl treatments. Additionally, while there were some differences in the metabolic pathways enriched in the roots and stems, both tissues commonly enriched pathways related to the biosynthesis of secondary metabolites, biosynthesis of cofactors, biosynthesis of amino acids, flavonoid biosynthesis, and ABC transporters.

Association analysis further indicated that biosynthesis of amino acids and plant hormone signal transduction pathway play key roles in the response of *P. talassica* × *P. euphratica* to salt stress. The interactions between the differentially expressed genes (DEGs) and several differentially accumulated metabolites (DAMs), especially the strong association between *LOC105124002* and Jasmonoyl-L-Isoleucine (pme2074), were again revealed by the interactions analysis.

*Correspondence:
Zhanyuan Lu
lzhy2811@163.com
Zhanjiang Han
hanzhanjiang@taru.edu.cn
Full list of author information is available at the end of the article

Conclusions In this study, we resolved the changes of metabolic pathways in roots and stems of *P. talassica* × *P. euphratica* under different NaCl treatments and explored the associations between characteristic DEGs and DAMs, which provided insights into the mechanisms of *P. talassica* × *P. euphratica* in response to salt stress.

Keywords *Populus. talassica* × *Populus. euphratica* seedlings, NaCl treatment, Differentially expressed genes (DEGs), Differentially accumulated metabolites (DAMs), Metabolic pathways

Background

About 20% of the world's arable land is severely damaged by salinisation, and the remaining half is affected to varying degrees [1]. In China, approximately 99.13 million hectares of land are affected by salinity and alkalinity, with Xinjiang alone accounting for 21.81 million hectares of this area [2, 3]. Located in the arid and semi-arid northwest of China, Xinjiang experiences a temperate continental climate characterized by low rainfall and high evapotranspiration.

Due to prolonged drip irrigation under mulch, inadequate salt leaching has caused soil salinization in Xinjiang, where the pH exceeds 8.0. Approximately one-third of the arable land is affected, and the low utilization of this land significantly hinders agricultural development [4–8]. Soil salinity, a key abiotic stress, restricts plant growth and leads to significant yield reductions globally [9]. Salt stress can inhibit plant growth and impair plant development at several physiological, hormonal and metabolic levels [10]. NaCl is the most soluble and abundant salt among various types, and it is the primary salt released into the soil, which is the most important salt in nature and the main component causing salt stress [11]. In recent years, it has been reported that major grain crops (rice, wheat and maize) cannot even complete their reproductive life span when salt concentration in soil exceeds 200 mM [12]. Saline plants, which are adapted to saline conditions, can tolerate high salt concentrations and may even thrive under such conditions for optimal growth [13]. They can survive and reproduce in 200 mM NaCl or higher salt concentrations [14].

The Xinjiang Forestry Academy of Sciences has developed a new variety of *Populus talassica* (♀) × *Populus euphratica* (♂) through cross-breeding between *P. euphratica* and *P. talassica* over a period of 36 years, and it passed the National Seed Validation in 2009. *P. talassica* × *P. euphratica* has a significant hybrid advantage, and its resistance is markedly higher than that of the maternal parent *P. talassica*, and close to that of the paternal parent *P. euphratica*. Under the harsh environment, *P. talassica* × *P. euphratica* shows the excellent characteristics of *P. euphratica*, such as drought resistance, barrenness resistance, cold resistance, and salinity resistance, etc. At the same time, it inherits the advantages of *P. talassica*, such as fast growth, straight stem, and excellent material. As an excellent tree species with great potential, *P. talassica* × *P. euphratica* shows wide application value in landscape greening, ecological management, and windbreaks and sand control afforestation in arid, saline, and sandy areas.

Studies have shown that *P. talassica* × *P. euphratica* can grow normally on strong saline and alkaline land with a pH of 9.46 and total salt content of 1.5–2.4%, and its success rate of cuttings propagation is as high as 94% [15, 16]. The saline soil in the Tarim Basin has a large area with significant differences in salt content, and the planting of the highly resistant *P. talassica* × *P. euphratica* is of great value for the ecological management of saline and alkaline soils [17, 18].

Recent advancements in high-throughput technologies have made it faster and more cost-effective to obtain transcriptomic and metabolomic data, which not only advances the understanding of molecular regulatory mechanisms and metabolic networks in plants, but also provided new perspectives for studying the adaptive mechanisms of plants under adversity conditions [19]. For example, a vast array of studies have been carried out on the molecular mechanisms of plant response to salt stress using transcriptomic and metabolomic analysis techniques. High-throughput sequencing has allowed researchers to gain initial insights into the molecular mechanisms involved in plant responses to salt stress [20, 21]. Therefore, with the increasing severity of soil salinity and the rapid development of high-throughput technology, it is particularly important to study the salt tolerance mechanisms of *P. talassica* × *P. euphratica*. Previous field experiments have proved that salt stress has a considerable effect on both morphological characteristics and physiological properties of *P. talassica* × *P. euphratica*, but the signal transduction pathways and regulatory mechanisms in reaction with salt stress are currently unknown. To clarify the reaction mechanisms of the saline plant *P. talassica* × *P. euphratica*, this study aimed to identify key pathways, DEGs, and DAMs involved in salt stress. Transcriptomic sequencing and comprehensive targeted metabolomic analysis were performed on *P. talassica* × *P. euphratica* under various NaCl treatments. The transcriptomic analysis was performed and published elsewhere in *Genes* [22]. In this research, we investigated the integrated response of *P. talassica* × *P. euphratica* to salt

stress, with a view to enhancing the growth performance and adaptive capacity of the crop under salt stress conditions, and thus improving the crop's salt tolerance. It will open up new ways for crop resistance cultivation and efficient production, as well as provide ideas and data to support for crop genetic improvement.

Materials and methods

Plant material and cultivation parameters

The research was implemented at the seedling base of the 10th Regiment, 1st Division of the Xinjiang Production and Construction Corps (81°15′32.64″E, 40°34′6.14″N), at an altitude of 1014 m. The region experiences a warm-temperate extreme continental arid desert climate, with peak temperatures reaching 35 °C and minimum temperatures dropping to −28 °C. The annual average sunshine duration ranges from 2,556.3 to 2,991.8 h. Precipitation is limited, snowfall during winter is infrequent, and surface evaporation is relatively high. The annual precipitation varied between 40.1 mm and 82.55 mm, while the annual evaporation ranged from 1876.6 mm to 2558.9 mm.

One-year-old potted seedlings of *P. talassica*×*P. euphratica* with heights ranging from 79 to 92 cm, were selected for the experiment. The experiment was implemented in open pots with loamy soil, soil pH of 7.9, soil salinity of 0.49 g/kg, soil density of 1.36 g/cm^3, soil conductivity of 852.6 μs/cm, soil organic matter content of 21.04 g/kg, and soil effective potassium content of 148.96 mg/kg. The soil fast-acting phosphorus and alkaline nitrogen contents were 7.49 mg/kg and 139.58 mg/kg, respectively.

Salt treatment and sample collection

A completely randomised design was used for the trial. The basal salinity of the potting soil served as the control and the seedlings were treated as follows: (a) control (CK: 0 mM NaCl); (b) low concentration (200 mM NaCl); and (c) high concentration (400 mM NaCl). The concentration levels were selected and adjusted according to prior research on salt tolerance in *P. talassica*×*P. euphratica* [17]. Forty-five potted seedlings with the same growth trend and free of pests and diseases were selected. Three biological replicates were set up for each treatment, with five plants in each replicate. One liter of NaCl solution with equal concentration was watered each time in the treatment group, while the CK group received an equal amount of deionized water. A tray was set under the pots for collecting exudates, which were then poured back into the pots after exudation, and the specific planting plot settings and NaCl concentration treatments can be found in Fig. 1.

The NaCl treatment was administered every three days for a total of five applications until the target concentration was achieved, and the NaCl concentration in the pots remained stable thereafter. Under the same growth conditions, the morphological and physiological indexes of *P. talassica*×*P. euphratica* were measured on the second day after the 15th, 30th and 45th days of NaCl treatment. Root and stem samples of *P. talassica*×*P. euphratica* seedlings were collected simultaneously and quickly snap-frozen in liquid nitrogen. The samples were then stored at −80 °C in an ultra-low temperature freezer for subsequent histological analysis.

Morphological and physiological indicators

Three seedlings each from the treatment and CK groups, for a total of 9 seedlings, were carefully excavated along with their root systems. Following excavation, the plants were transferred to the laboratory and rinsed with deionized water. The root-to-shoot ratio were then measured using the oven-drying and weighing method [23]. For detailed methods, please refer to the supplementary materials.

Three well-grown and healthy *P. talassica*×*P. euphratica* seedlings, totalling nine plants, were selected in each treatment group on the second day after the 15th, 30th and 45th days of NaCl treatment. The root portion of the plants was selected and RWC of the root system was determined using the drying and weighing method [24]. For detailed methods, please refer to the supplementary materials.

Methods of histological analysis

Histological sample information and test materials, methods

The grouping of each sample in the roots and stems of *P. talassica*×*P. euphratica* in the CK and NaCl-treated groups and the corresponding information is shown in Table 1.

Transcriptomic analysis

The transcriptomic analysis was performed and published elsewhere in *Genes* [22], please refer to the supplementary material for specific methods.

Metabolomic analysis

Sample extraction process

The biological samples were freeze-dried, ground into powder, and extracted with 70% methanol. After vortexing and centrifugation, the samples were filtered through a 0.22 μm membrane, and stored in injection vials for UPLC-MS/MS analysis. For detailed methods, please refer to the supplementary materials.

Chromatography and mass spectrometry acquisition conditions

The data acquisition system was primarily composed of Ultra Performance Liquid Chromatography coupled with

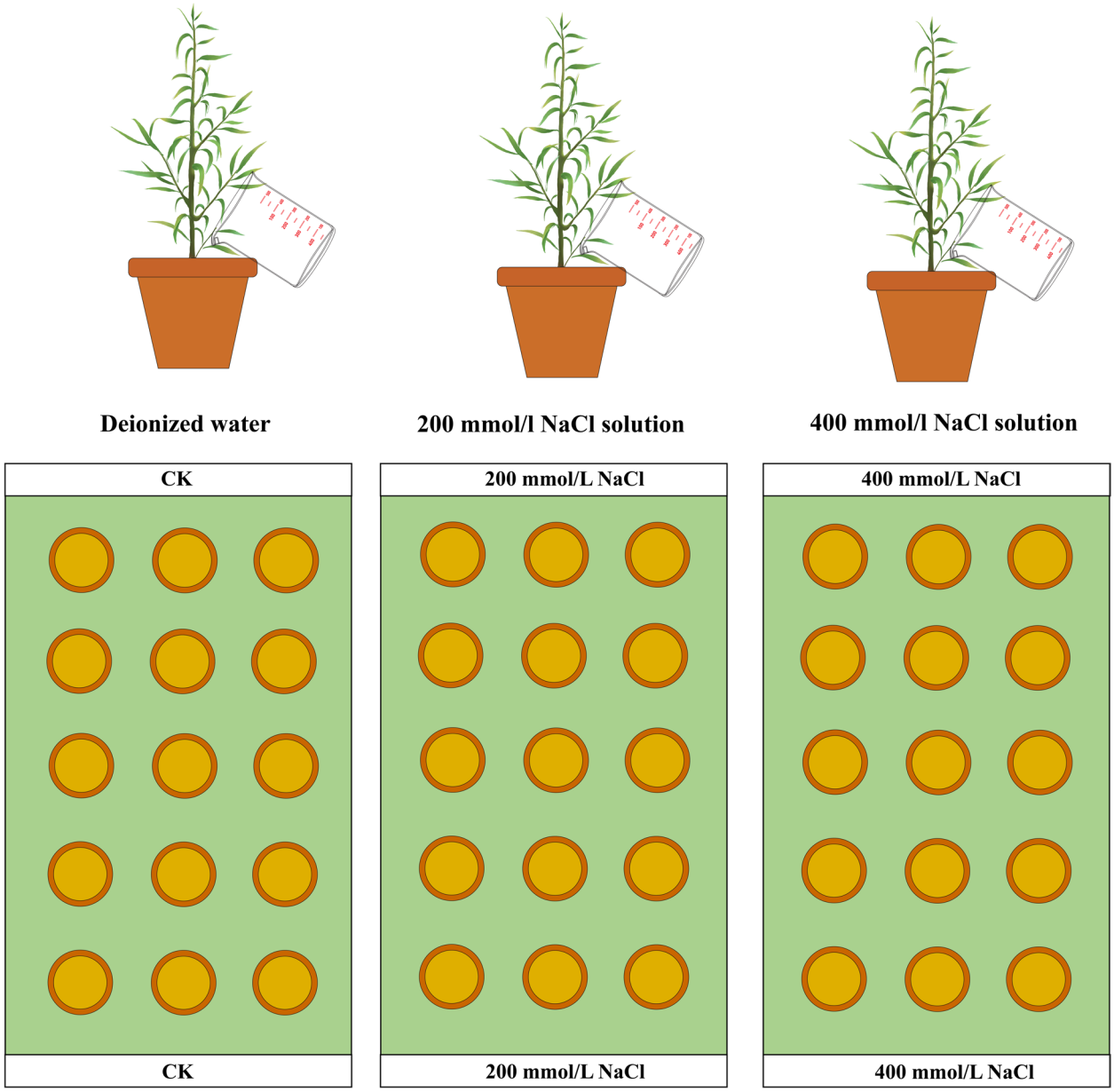

Fig. 1 *P. talassica* × *P. euphratica* planting set-up and NaCl treatments

Tandem Mass Spectrometry. The liquid chromatography conditions included an Agilent SB-C18 column, a gradient of ultrapure water (0.1% formic acid) and acetonitrile (0.1% formic acid), a flow rate of 0.35 mL/min, column temperature at 40 °C, and an injection volume of 2 μL. MS conditions mainly include: ESI source at 500 °C, ion spray voltage of 5500 V (positive) / −4500 V (negative), gas pressures at 50, 60, and 25 psi, with MRM mode scanning and optimized DP and CE. For detailed methods and procedures, please refer to the supplementary materials.

Principal component analysis (PCA) of the overall sample and cluster analysis of the sample

In this study, PCA was conducted on the samples, including QC samples, to assess the general metabolic differences between sample groups and the variability within each group. Heatmaps were created with the ComplexHeatmap package in R software, and hierarchical clustering analysis was employed to assess the metabolite accumulation patterns across different samples.

Table 1 Sample grouping information table of *P. talassica* × *P. euphratica*

Species	Organizational Parts	Sample Name	Group
P.talassica × *P.euphratica*	stem	SCK-1	SCK
P.talassica × *P.euphratica*	stem	SCK-2	SCK
P.talassica × *P.euphratica*	stem	SCK-3	SCK
P.talassica × *P.euphratica*	stem	S200-1	S200
P.talassica × *P.euphratica*	stem	S200-2	S200
P.talassica × *P.euphratica*	stem	S200-3	S200
P.talassica × *P.euphratica*	stem	S400-1	S400
P.talassica × *P.euphratica*	stem	S400-2	S400
P.talassica × *P.euphratica*	stem	S400-3	S400
P.talassica × *P.euphratica*	root	RCK-1	RCK
P.talassica × *P.euphratica*	root	RCK-2	RCK
P.talassica × *P.euphratica*	root	RCK-3	RCK
P.talassica × *P.euphratica*	root	R200-1	R200
P.talassica × *P.euphratica*	root	R200-2	R200
P.talassica × *P.euphratica*	root	R200-3	R200
P.talassica × *P.euphratica*	root	R400-1	R400
P.talassica × *P.euphratica*	root	R400-2	R400
P.talassica × *P.euphratica*	root	R400-3	R400

Screening of key DAMs for salt tolerance

To identify key DAMs potentially associated with salt tolerance in *P. talassica* × *P. euphratica*, we used $|\log_2$ (fold change)$| > 2.0$ or $|\log_2$ (fold change)$| < 0.5$, VIP > 1.0, and *P*-value < 0.05 as screening criteria for significant DAMs. A number of key DAMs with high abundance were screened from the list of DAMs in each comparison group of roots and stems.

Functional annotation and pathway enrichment analysis of DAMs

Metabolites interact to establish various pathways within the organism. Metabolites were mapped to the KEGG database, showing only metabolic pathways containing DAMs [25]. KEGG pathway enrichment analysis was performed based on the DAMs results. The top 20 pathways, ranked by their *P*-value from smallest to largest, were selected and presented. The DAMs were aligned with the KEGG database to retrieve the enrichment results for their respective metabolic pathways [26].

Statistical analysis of data and construction of metabolic networks

MS data were analysed by Chroma TOF 4.3x (LECO) for peak extraction, baseline correction, deconvolution, peak integration, and peak alignment, with qualitative analysis of the compounds performed using the LECO-Fiehn Rtx5 database [27]. The normalized data were further processed with SIMCA 14.1 (Umea, Sweden) software, which included logarithmic transformation, centering, and PCA. Data were processed using Microsoft Office Excel 2007, GraphPad Prism 5, and IBM SPSS Statistics 25, with image adjustments made in Adobe Photoshop CS3 Extended.

Results

Morphological characteristics and physiological characterisation

Analysis of biomass and root-shoot ratio of P. talassica × *P. euphratica seedlings treated with varying NaCl concentrations*

Under salt stress conditions, saline plants adapted to different salt stresses by regulating the biomass allocation between aboveground and belowground parts. According to Table 2, the aboveground, belowground and whole plant biomass, as well as the root-shoot ratio of *P. talassica* × *P. euphratica* were basically the same before NaCl treatment.

The aboveground, underground, and total biomass of *P. talassica* × *P. euphratica* increased on the second day after the 15th, 30th and 45th days of 200 mM NaCl treatment compared to the control group. The root-shoot ratio on the second day after the 15th day of 200 mM NaCl treatment was slightly lower than that of the control. However, while on the second day after the 30th and 45th days of 200 mM NaCl treatment, the root-shoot ratio were markedly greater than those of the control group ($P < 0.05$). As the NaCl concentration reached 400 mM, the aboveground, underground and total biomass and root-shoot ratio were markedly lower than CK group on the second day after the 15th, 30th, and 45th days of NaCl treatment, and the decrease was particularly significant at the 45th day ($P < 0.05$).

The results showed that 200 mM NaCl treatment promoted the biomass accumulation of *P. talassica* × *P. euphratica* seedlings to some degree, while 400 mM NaCl treatment markedly reduced biomass (Table 2). These results indicate that when salt stress reaches a significant level, low concentrations of NaCl treatment can promote the growth of aboveground and belowground parts, thus increasing the biomass accumulation of *P. talassica* × *P. euphratica* seedlings and leading to an increase in root-shoot ratio. In contrast, high concentrations of salt stress inhibited the growth of belowground parts, which in turn led to a decrease in root-shoot ratio (Table 2).

Table 2 Effects of different NaCl treatments on biomass and root-shoot ratio

NaCl concentration (mM)	Time period	Above-ground biomass (g)	Below-ground biomass (g)	Total plant biomass (g)	Root-shoot ratios
CK	0 d	17.98 ± 0.04a	8.12 ± 0.02a	26.10 ± 0.03a	0.45 ± 0.00a
	15 d	19.54 ± 0.29f	10.63 ± 0.14d	30.17 ± 0.43e	0.54 ± 0.01d
	30 d	22.32 ± 0.10d	12.10 ± 0.08c	34.42 ± 0.17d	0.54 ± 0.01d
	45 d	25.24 ± 0.11b	14.07 ± 0.04b	39.31 ± 0.14b	0.56 ± 0.01c
200 mM NaCl	0d	17.98 ± 0.03a	8.12 ± 0.01a	26.10 ± 0.03a	0.45 ± 0.00a
	15 d	20.26 ± 0.15e	10.25 ± 0.16e	30.51 ± 0.31e	0.51 ± 0.01e
	30 d	24.37 ± 0.28c	14.02 ± 0.13b	38.39 ± 0.40c	0.57 ± 0.01b
	45 d	30.01 ± 0.58a	19.42 ± 0.51a	49.43 ± 1.08a	0.65 ± 0.01a
400 mM NaCl	0 d	18.00 ± 0.02a	8.11 ± 0.02a	26.11 ± 0.03a	0.45 ± 0.00a
	15 d	17.89 ± 0.06 h	8.44 ± 0.05 h	26.33 ± 0.11 g	0.47 ± 0.01 g
	30 d	18.11 ± 0.06 h	8.78 ± 0.04 g	26.89 ± 0.10 g	0.48 ± 0.01f
	45 d	18.58 ± 0.04 g	9.34 ± 0.02f	27.92 ± 0.06f	0.50 ± 0.01e

Note: Data in this table are mean ± standard deviation, and different lowercase letters indicate statistically significant differences ($p < 0.05$)

Observation of root phenotypes and determination of the RWC of P. talassica × P. euphratica under different NaCl treatments

Root phenotypes of *P. talassica* × *P. euphratica* seedlings were observed on the second day after the 45th day of NaCl treatment at different concentrations. The results showed significant phenotypic differences between the CK group, the 200 mM and 400 mM NaCl-treated groups, indicating that the NaCl treatment reached a significant level. Furthermore, 200 mM NaCl treatment markedly promoted the increase in root length, root surface area, and count of root tillers in the root system of *P. talassica* × *P. euphratica* seedlings (Fig. 2A).

Subsequently, the RWC of *P. talassica* × *P. euphratica* seedlings was determined on the second day after the 15th, 30th, and 45th days of NaCl treatment with different concentrations. On the second day after the 45th day of 200 mM NaCl treatment, the roots RWC was markedly lower than the 15th day, with an average value of approximately 81%. Marked differences in the RWC of the roots were observed on the second day after the 15th, 30th, and 45th days of 400 mM NaCl treatment ($P < 0.05$). The RWC of the roots decreased to the lowest on the second day after the 45th day of 400 mM NaCl treatment, with an average value of about 75%. These results showed that the roots RWC of *P. talassica* × *P. euphratica* gradually decreased with increasing NaCl concentration, with the most pronounced decrease observed under 400 mM NaCl treatment, especially on the second day after the 45th day of salt treatment (Fig. 2B).

Transcriptomic analysis

DEGs analysis in P. talassica × P. euphratica under varying NaCl concentrations

Among the comparison groups for the roots and stems of *P. talassica* × *P. euphratica*, the RCK_vs_R400 and SCK_vs_S400 groups had the highest number of DEGs. The number of DEGs in both roots and stems were markedly higher than in the control group with increasing NaCl concentration. This indicated that salt treatment markedly increased the expression of DEGs in the roots and stems of *P. talassica* × *P. euphratica* (Fig. 3).

KEGG pathway enrichment analysis of DEGs under different NaCl concentrations

KEGG pathway enrichment analysis of DEGs enriched in roots and stems revealed that plant hormone signal transduction, phenylpropanoid biosynthesis were found in RCK_vs_R200, RCK_vs_R400 and R200_vs_R400 comparator groups, MAPK signaling pathway—plant, plant-pathogen interaction and ABC transporters were all enriched with more DEGs in the pathway (Fig. 4). While in the SCK_vs_S200, SCK_vs_S400 and S200_vs_S400 comparison groups, glycolysis / gluconeogenesis, plant-pathogen interaction, MAPK signaling pathway—plant, plant hormone signal transduction, carbon metabolism, biosynthesis of amino acids and pyruvate metabolism were all enriched with more DEGs in the pathways. DEGs in the pathways of plant hormone signal transduction, plant-pathogen interaction and MAPK signaling pathway—plant were markedly enriched in both roots and stems of *P. talassica* × *P. euphratica*.

In roots, DEGs were enriched in multiple pathways and, unlike stems, DEGs in roots were also markedly enriched in nitrogen metabolism, terpenoid backbone biosynthesis, phenylalanine, tyrosine and tryptophan biosynthesis, ABC transporters, galactose metabolism, glycosphingolipid metabolism and sphingolipid metabolism pathways. In addition, DEGs from stems showed significant enrichment in carbon metabolism, carbon fixation in photosynthetic organisms, 2-oxocarboxylic acid

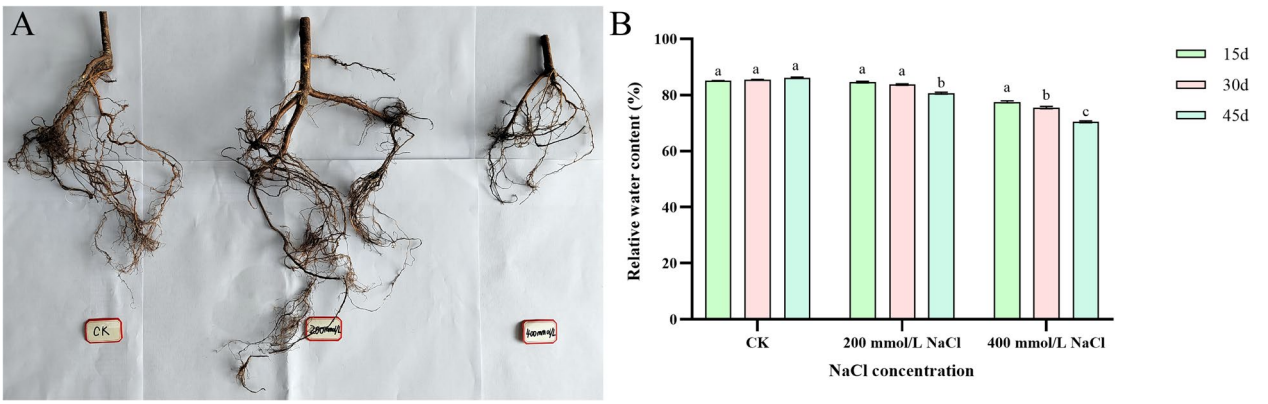

Fig. 2 Observation of root phenotype and determination of RWC. **A** Phenotypic observation of root system of *P. talassica* × *P. euphratica* on the second day after the 45th day of NaCl treatment with different concentrations. **B** Determination of RWC of root system of *P. talassica* × *P. euphratica* under different NaCl concentrations. Note: Letters a, b, and c above the graphs indicate statistically significant differences between groups ($p < 0.05$) with a 95% confidence level that the differences between groups are reliable. The interpretation of minimal bias is that these significant differences are real and not due to random error

metabolism, pyruvate metabolism, glycine, serine and threonine metabolism, biosynthesis of unsaturated fatty acids and lysine biosynthesis pathways were also markedly enriched, whereas DEGs in roots were not enriched in these pathways (Fig. 4). The above results revealed the existence of different response mechanisms in the roots and stems of *P. talassica* × *P. euphratica* in reaction with salt stress.

Screening of key DEGs for salt tolerance

Significant DEGs in the roots and stems of *P. talassica* × *P. euphratica* were identified using the criteria $|\log_2$ fold change$| \geq 5$ and padj < 0.01. A total of 14 significant DEGs were found across the three comparison groups of the stems, with detailed gene information provided in supplementary Table 4 of supplementary material. In the SCK_vs_S200 comparison group, the DEGs with higher expression levels such as *LOC105119414* belongs to the AP2/ERF TF family, *LOC105142033* belongs to the NAC protein family, and *LOC105119522* belongs to the WRKY TF family. In the SCK_vs_S400 comparison group, the DEGs with higher expression levels such as *LOC105126640* belongs to the ocs element-binding factor 1-like TF, which binds to the octopine synthase element in plants, and *LOC105131256* belongs to the WRKY TF family. In the S200_vs_S400 comparison group, the DEGs with higher expression levels such as *LOC105116962* belongs to the NAC protein family, *LOC105115491* belongs to the WRKY TF family, *LOC105134677* belongs to the ocs element-binding factor 1-like family, and *LOC105134493* belongs to the R2R3- MYB TF family.

A total of 14 significant DEGs were screened in the three comparison groups of *P. talassica* × *P. euphratica* roots, and the specific gene information provided in supplementary Table 4 of supplementary material. In the RCK_vs_R200 comparison group, the DEGs exhibiting higher expression levels such as *LOC105108844* belongs to the ERF subfamily of the AP2/ERF superfamily, *LOC105135115* belongs to the NAC protein family, *LOC105114369* belongs to the WRKY TF family, and both *LOC105134637* and *LOC105115176* belong to the bZIP transcription factor family. In the RCK_vs_R400 comparison group, the DEGs with higher expression levels such as *LOC105127231* belongs to the JUNGBRUNNEN 1-like TF, which is strongly associated with antioxidant defense and the reaction to environmental stresses in plants, *LOC105107217* is a member of the ERF subfamily of the AP2/ERF superfamily, *LOC105124330* belongs to the WRKY TF family, *LOC105115119* belongs to the bZIP family of TFs, and *LOC105128502* belongs to the ocs element-binding factor 1-like TF family.

In the R200_vs_R400 comparison group, the DEGs with higher expression levels such as *LOC105120059* belongs to the DREB TF family, *LOC105116469* belongs to the NAC TF family, *LOC105127348* belongs to the WRKY TF family, and *LOC105124801* belongs to bZIP TF family. The summary of the above results showed that most of the significant DEGs from *P. talassica* × *P. euphratica* stems belonged to the AP2/ERF, NAC protein family, WRKY, R2R3-MYB, and ocs element-binding factor 1-like TFs. In roots, most of the prominent DEGs belonged to the AP2/ERF, NAC protein family, bZIP, WRKY, JUNGBRUNNEN 1-like transcription factor, and ocs element-binding factor 1-like families. DEGs from the bZIP, DREB and JUNGBRUNNEN 1-like TFs were also present in *P. talassica* × *P. euphratica* roots compared to stems. In contrast, compared to the roots, *P.*

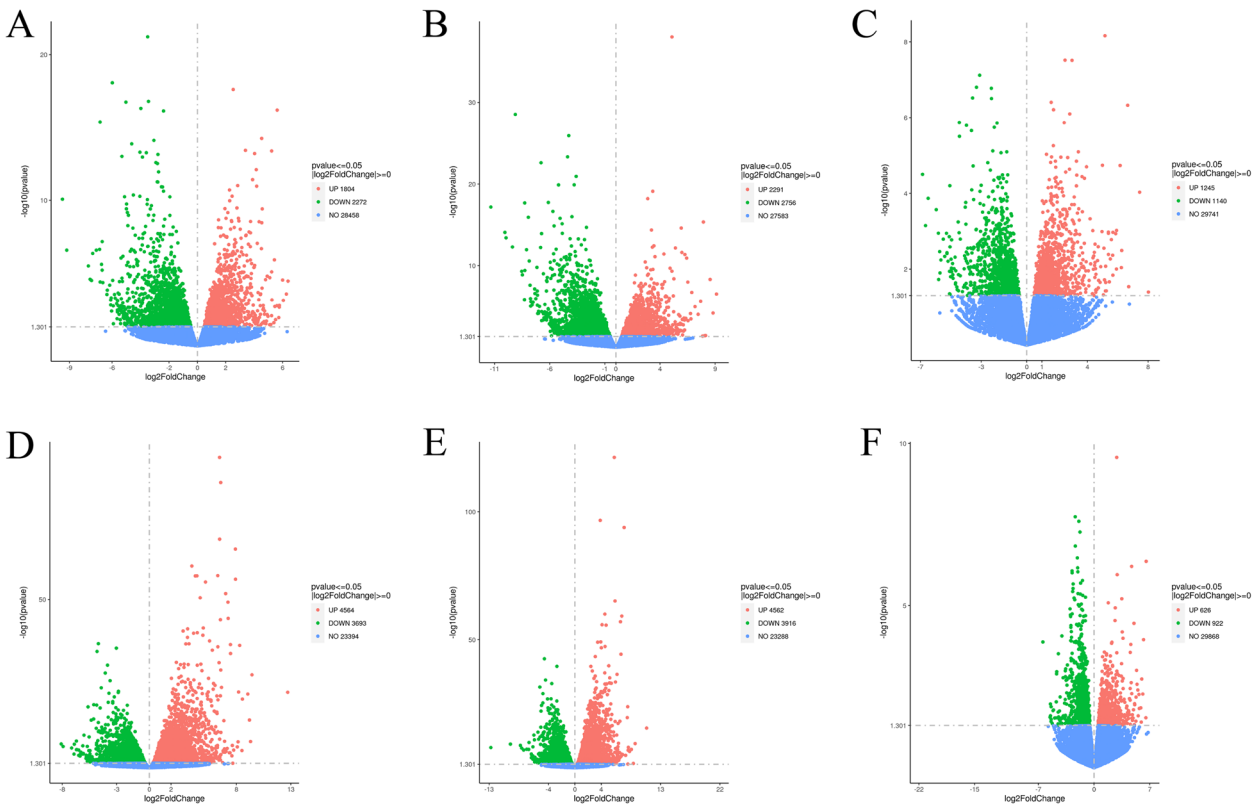

Fig. 3 Volcanic maps of DEGs in various comparative groups of roots and stems. **A** RCK_vs_R200. **B** RCK_vs_R400. **C** R200_vs_R400. **D** SCK_vs_S200. **E** SCK_vs_S400. **F** S200_vs_S400

talassica×*P. euphratica* stems were enriched in DEGs of the R2R3-MYB transcription factor family. These results suggest that there are significant differences in gene expression patterns between roots and stems. The transcriptomic analysis was performed and published elsewhere in *Genes* [22].

Metabolomic analysis

To explore the metabolite enrichment and the metabolic pathways that are markedly affected in the roots and stems of *P. talassica*×*P. euphratica* under salt stress, we conducted metabolomic analysis on seedlings subjected to different concentrations of NaCl treatments.

Quantitative analysis of DAMs

In this study, a total of 1,298 metabolites were identified using the UPLC-MS/MS platform in combination with a self-constructed database. Table 3 presents the statistical results for the number of DAMs in the root and stem comparison groups of *P. talassica*×*P. euphratica.* The findings indicated that 105 DAMs were detected in the comparison group of RCK_vs_R200, 66 DAMs in the comparison group of RCK_vs_R400, and 93 DAMs in the comparison group of R200_vs_R400. In the comparison group of stems, 35 DAMs were recognized in the comparison group of SCK_vs_S200, SCK_vs_S400 detected 84 DAMs, and the S200_vs_S400 comparison group detected 69 DAMs (Table 3).

The results showed that the number of DAMs in the RCK_vs_R200 comparison group was the highest among the comparison groups of *P. talassica*×*P. euphratica* roots. Among the comparison groups of stems, the SCK_vs_S400 comparison group had the highest number of DAMs, and the DAMs of both comparison groups were predominantly downregulated. It was further demonstrated that the upregulated and downregulated DAMs markedly increased in the roots of *P. talassica*×*P. euphratica* under 200 mM NaCl treatment. However, the number of both upregulated and downregulated DAMs in the roots markedly decreased when the NaCl concentration reached 400 mM (Table 3). In contrast, the amounts of upregulated and downregulated DAMs in the stems of *P. talassica*×*P. euphratica* consistently increased with the rising NaCl concentration. These results suggest that DAMs in roots and stems of *P. talassica*×*P. euphratica* exhibit different trends under saline conditions.

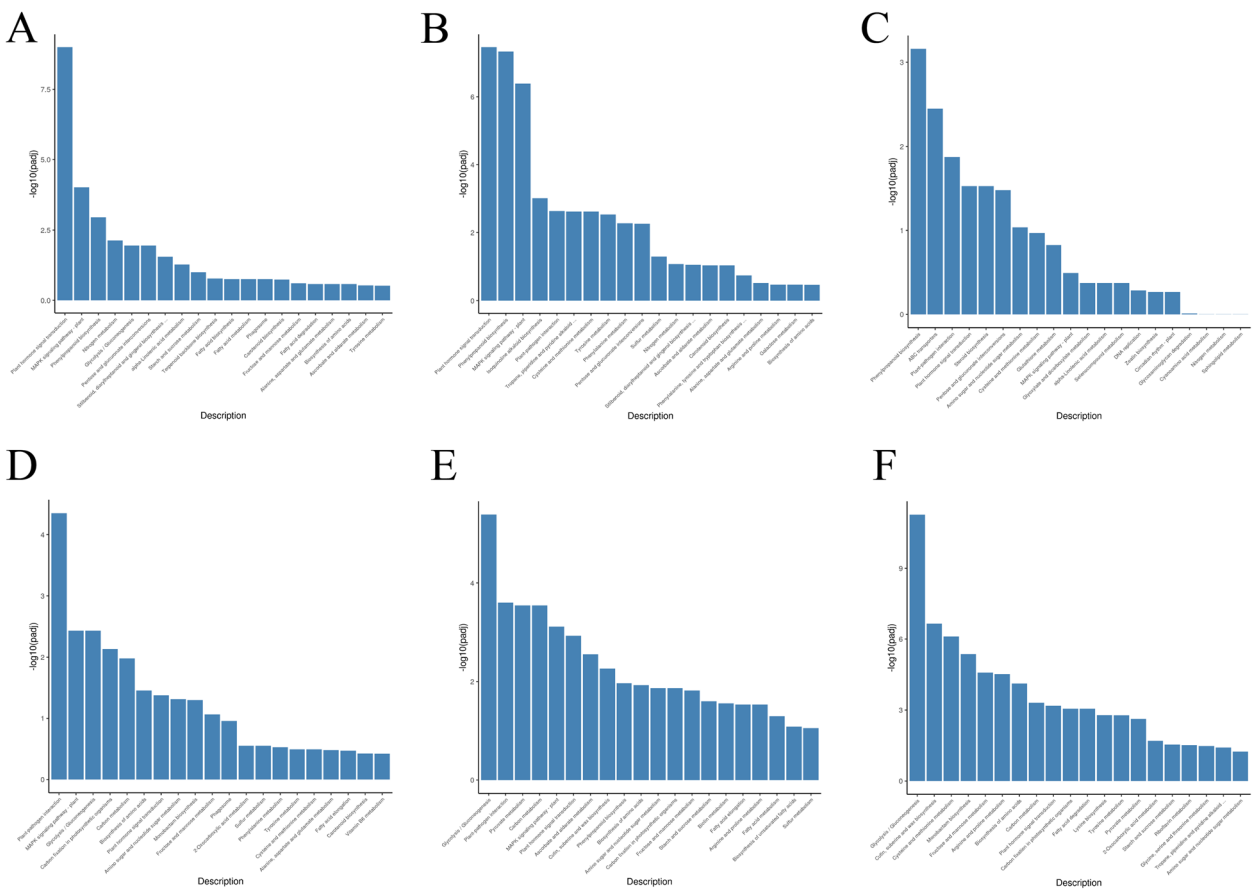

Fig. 4 KEGG bars of DEGs in various comparative groups of roots and stems. **A** RCK_vs_R200. **B** RCK_vs_R400. **C** R200_vs_R400. **D** SCK_vs_S200. **E** SCK_vs_S400. **F** S200_vs_S400

PCA of metabolites, category composition analysis, and cluster analysis of samples as a whole

The PCA plot (Fig. 5A) demonstrated the differences in metabolite distribution among different treatment groups. PC1 contributed 48.19%, while PC2 contributed 7.82%, with a clear separation trend. And the points of SCK and S200 and S400 groups were clustered in the left region on both PC1 and PC2 axes, while the RCK, R200 and R400 groups were clustered in the right region. This clustering reflected that samples within each group exhibited similarity, while the metabolite distributions between different treatment groups were markedly different. Notably, the separation along PC1 was more obvious. The QC group points were clustered near the centre, indicating good quality and reproducibility (Fig. 5A). Using the UPLC-MS/MS assay platform and a self-constructed database, 1,298 metabolites were identified. The metabolites in the roots and stems of *P. talassica*×*P. euphratica* seedlings under salt stress were primarily composed of flavonoids (25.5%), phenolic acids (20.8%), lipids (9.01%), alkaloids (7.4%), amino acids and derivatives (7.24%), organic acids (5.39%), nucleotides and derivatives (5.16%), and lignans and coumarins (4.7%) (Fig. 5B).

Table 3 Table of the number of DAMs in *P. talassica*×*P. euphratica*

Group name	Total DAMs	Down regulated	Up regulated
RCK_vs_R200	105	69	36
RCK_vs_R400	66	45	21
R200_vs_R400	93	37	56
SCK_vs_S200	35	26	9
SCK_vs_S400	84	53	31
S200_vs_S400	69	21	48

Note: Group name: difference comparison group information; Total DAMs: number of metabolites with significant differences; Down regulated: number of downregulated metabolites; Up regulated: number of upregulated metabolites

The Pearson correlation coefficient was computed using the cor function in R software, where a value of |r| closer to 1 indicates a stronger correlation between replicates. As shown in Fig. 5C, the correlation among the three *P. talassica*×*P. euphratica* samples under different NaCl treatment conditions was low, but the correlation

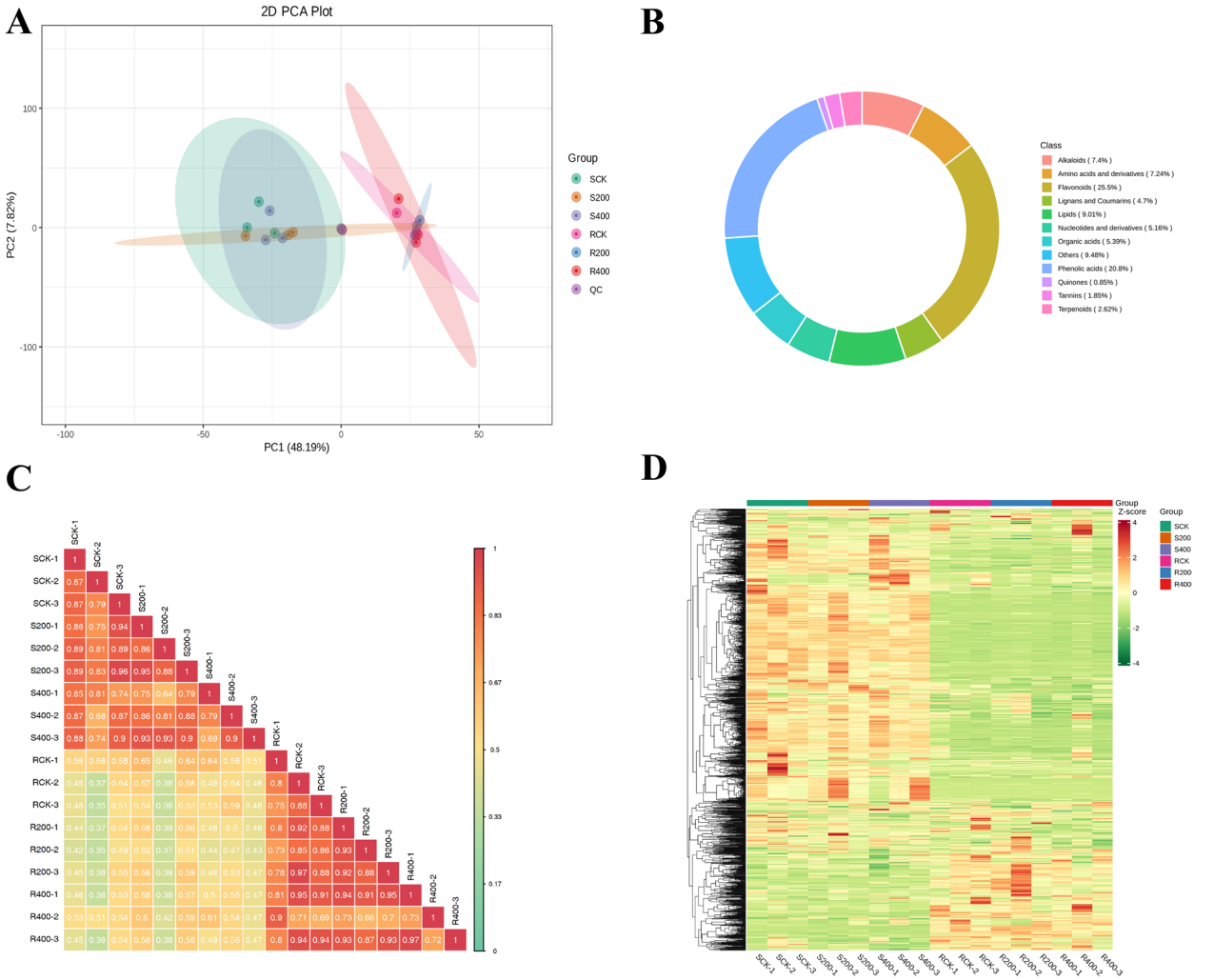

Fig. 5 Comparative metabolite classification of *P. talassica* × *P. euphratica* under salt stress. **A** PCA scores plot for each sample group versus MS data of quality control samples. **B** circular plot of metabolite class composition. **C** Inter-sample correlation analysis plot. **D** Overall sample clustering plot

among replicates was high, indicating that the correlation among samples under the same treatment conditions was high (Fig. 5C). To visualise the differences in metabolites of *P. talassica* × *P. euphratica* under different salt treatments, clustering heatmap analysis was conducted for diverse compounds. The results revealed the similarity relationship between root and stem samples and their corresponding comparative groups (Fig. 5D).

Dynamic distribution of metabolite content differences

To clearly illustrate the overall metabolic differences, the metabolite fold change (FC) values between the comparison groups were determined. The metabolite were then ranked from smallest to largest based on FC values. The differences in metabolite content distribution were visualized, with the top 10 DAMs showing up-regulation and down-regulation labeled accordingly.

As shown in Fig. 6, In the RCK_vs_R200, RCK_vs_R400, and R200_vs_R400 comparison groups, the markedly upregulated metabolite include flavonoids, phenolic acids, amino acids and derivatives, terpenoids, and organic acid analogs. The markedly downregulated metabolite are mainly flavonoids, phenolic acids, nucleotides and derivatives, and terpenoids. In the SCK_vs_S200, SCK_vs_S400, and S200_vs_S400 comparison groups, the markedly upregulated DAMs are primarily amino acids and derivatives, flavonoids, alkaloids, organic acids, and lipids. The markedly downregulated DAMs are primarily flavonoids, amino acids and derivatives, lipids, phenolic acids, alkaloids, and nucleotides and derivatives (Fig. 6).

Volcano diagram of DAMs

The criteria for identifying significant DAMs were $|\log_2$ (fold change)$| > 2.0$ or $|\log_2$ (fold change)$| < 0.5$, VIP > 1.0,

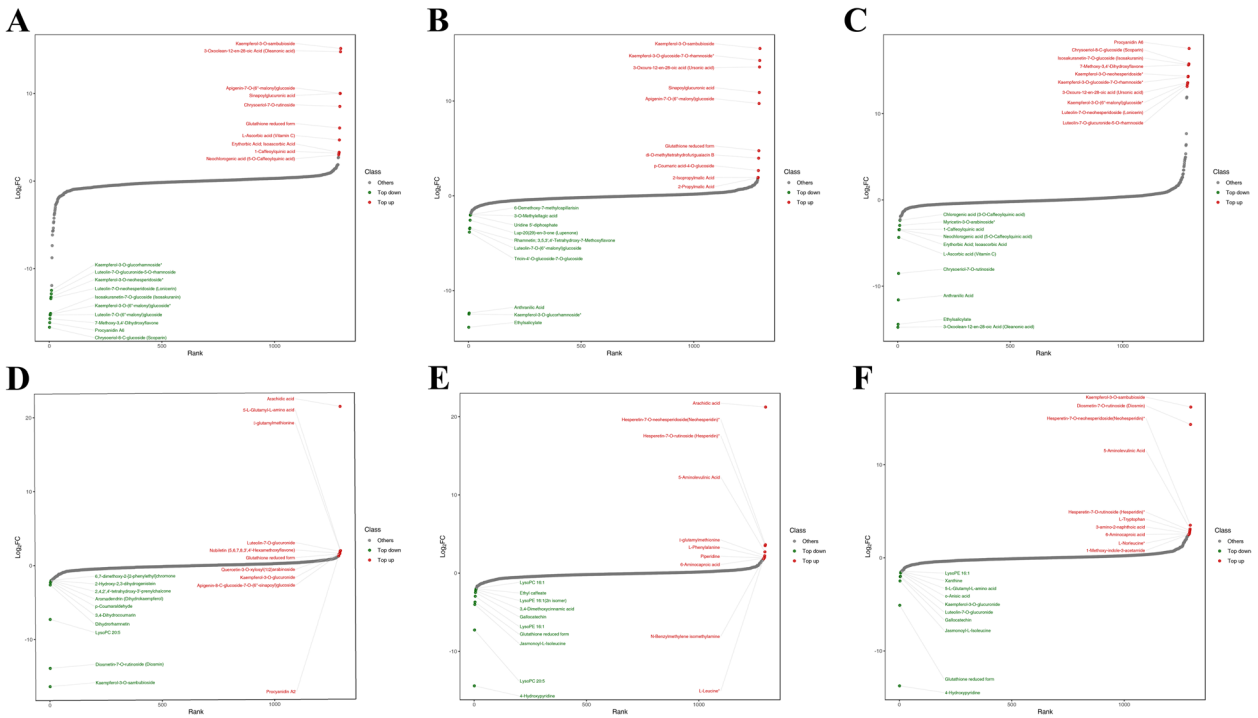

Fig. 6 Dynamic distribution of differences in metabolite content. **A** RCK_vs_R200. **B** RCK_vs_R400. **C** R200_vs_R400. **D** SCK_vs_S200. **E** SCK_vs_S400. **F** S200_vs_S400

and *P*-value < 0.05. A total of 73 significant DAMs were identified from the DAMs lists of each comparison group in the roots and stems, with the specific metabolite names presented in supplementary Table 2. As presented in supplementary Table 2, the markedly enriched DAMs were primarily DAMs in the categories of amino acids and derivatives, flavonoids, phenolic acids, nucleotides and derivatives, organic acids, and alkaloids.

Additionally, a volcano plot was generated based on the 73 significant DAMs identified (Fig. 7). The plot illustrates the distribution of DAMs in the roots and stems of *P. talassica*×*P. euphratica* seedlings under different NaCl concentrations. As seen in Fig. 7, a total of 29 significant DAMs were upregulated, and 44 significant DAMs were downregulated. In the RCK_vs_R200, RCK_vs_R400, and R200_vs_R400 comparison groups, 6, 5, and 3 DAMs were upregulated, and 10, 10, and 4 DAMs were downregulated, respectively. In the SCK_vs_S200, SCK_vs_S400, and S200_vs_S400 comparison groups, 3, 4, and 8 DAMs were upregulated, and 3, 14, and 3 DAMs were downregulated, respectively. Notably, the SCK_vs_S400 comparison group showed the highest number of significant DAMs, with downregulated DAMs predominating (Fig. 7).

The salt content was performed in real-time until the NaCl concentration increased to 200 mmol/L, the number of DAMs in the roots of *P. talassica*×*P. euphratica* markedly increased, while the number of DAMs in the stems slightly increased. As the NaCl concentration increased to 400 mM, the number of DAMs in the roots slightly decreased, while a significant increase was observed in the stems (Fig. 7). These results suggest that low salt treatment can increase the abundance of DAMs in the roots of *P. talassica*×*P. euphratica* to some extent, whereas high salt treatment may inhibit the accumulation of related DAMs in the roots. In contrast, the metabolite levels in the stems markedly increased when the NaCl concentration reached 400 mmol/L, highlighting distinct responses of the roots and stems to salt stress.

Heat map of DAMs clustering

To facilitate the observation of metabolites content changes, the original relative abundance of DAMs selected based on the screening standard, was processed row-wise with Unit Variance Scaling. A heatmap was then generated using the R software package, and the results are presented in Fig. 8. Cluster analysis revealed that NaCl treatment markedly altered the expression of DAMs in the roots and stems of *P. talassica*×*P. euphratica*. In the RCK_vs_R200 comparison group, the prominently clustered DAMs included flavonoids, phenolic acids, alkaloids, amino acids and derivatives, nucleotides and derivatives, and others. In the RCK_vs_R400

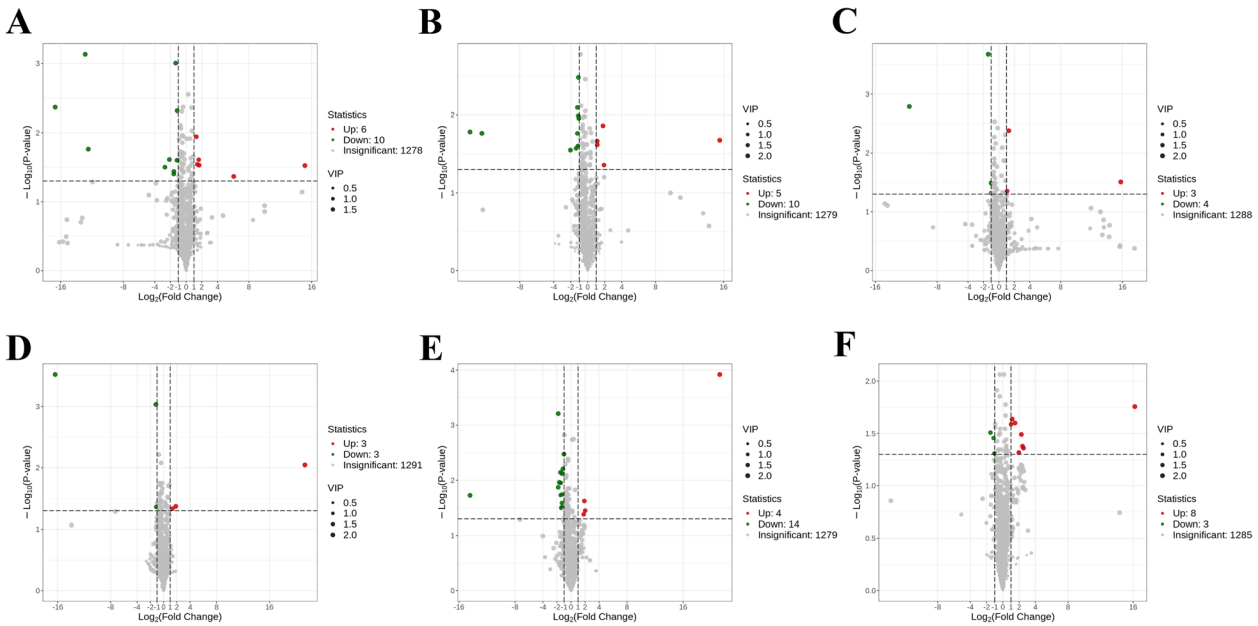

Fig. 7 DAMs volcano plot. **A** RCK_vs_R200. **B** RCK_vs_R400. **C** R200_vs_R400. **D** SCK_vs_S200. **E** SCK_vs_S400. **F** S200_vs_S400

comparison group, the prominent clustered DAMs mainly included flavonoids, phenolic acids, nucleotides and derivatives, amino acids and derivatives, alkaloids, and organic acids. In the R200_vs_R400 comparison group, the prominently clustered DAMs included flavonoids, phenolic acids, alkaloids, amino acids and derivatives, lignans and coumarins, and others (Fig. 8).

In the SCK_vs_S200 comparison group, the prominently clustered DAMs primarily include flavonoids, lipids, amino acids and derivatives, lignans and coumarins, alkaloids, and others. In the SCK_vs_S400 comparison group, the prominently clustered DAMs mainly consist of alkaloids, nucleotides and derivatives, amino acids and derivatives, flavonoids, organic acids, and phenolic acids. In the S200_vs_S400 comparison group, the prominently clustered DAMs primarily include alkaloids, amino acids and derivatives, flavonoids, nucleotides and derivatives, phenolic acids, and lipids. The DAMs common to the SCK_vs_S200, SCK_vs_S400, and S200_vs_S400 comparison groups include amino acids and derivatives, flavonoids, and alkaloids, suggesting that these DAMs may serve as universal physiological factors in *P. talassica*×*P. euphratica* under various stress conditions (Fig. 8).

K-means cluster analysis of DAMs

The results of the K-means clustering analysis revealed that these trends could be grouped into eight distinct categories (subclasses 1–8) in Fig. 9A. In these clusters, DAMs enriched due to NaCl treatment. The findings showed that the expression trend of DAMs content in class 7 exhibited a consistent decline as salt concentration increased, while the DAMs content in class 5 exhibited a pattern of initial increase followed by a subsequent decline. Additionally, and the metabolite content in class 6 and class 8 showed a downward trend followed by an upward trend. The DAMs were better reflected in clusters 1–8, with a total of 48, 80, 47, 41, 23, 34, 29, and 29 DAMs clustered in classes 1–8, respectively. In summary, cluster 2 contained the highest number of DAMs, while cluster 5 had the lowest number of DAMs (Fig. 9A).

The DAMs Venn diagram

The relationships between DAMs in the CK and NaCl-treated groups were presented in the form of Venn diagrams, and relationships between co-enriched and exclusive DAMs across all comparative groups. The results are shown in Fig. 9B. As shown in Fig. 9B, the two comparison groups exhibited a greater overlap of co-enriched DAMs, while the four comparison groups showed fewer overlapping DAMs. Additionally, many co-enriched DAMs varied between the comparison groups.

Under salt stress, the RCK_vs_R200, RCK_vs_R400, SCK_vs_S200, and SCK_vs_S400 groups, the RCK_vs_R400, R200_vs_R400, SCK_vs_S400, S200_vs_S400 group, and the RCK_vs_R200, R200_vs_R400, SCK_vs_S200, and S200_vs_S400 groups had 0, 2, and 1 co-varying DAMs, respectively. The number and expression trends of DAMs in roots and stems of *P. talassica*×*P.*

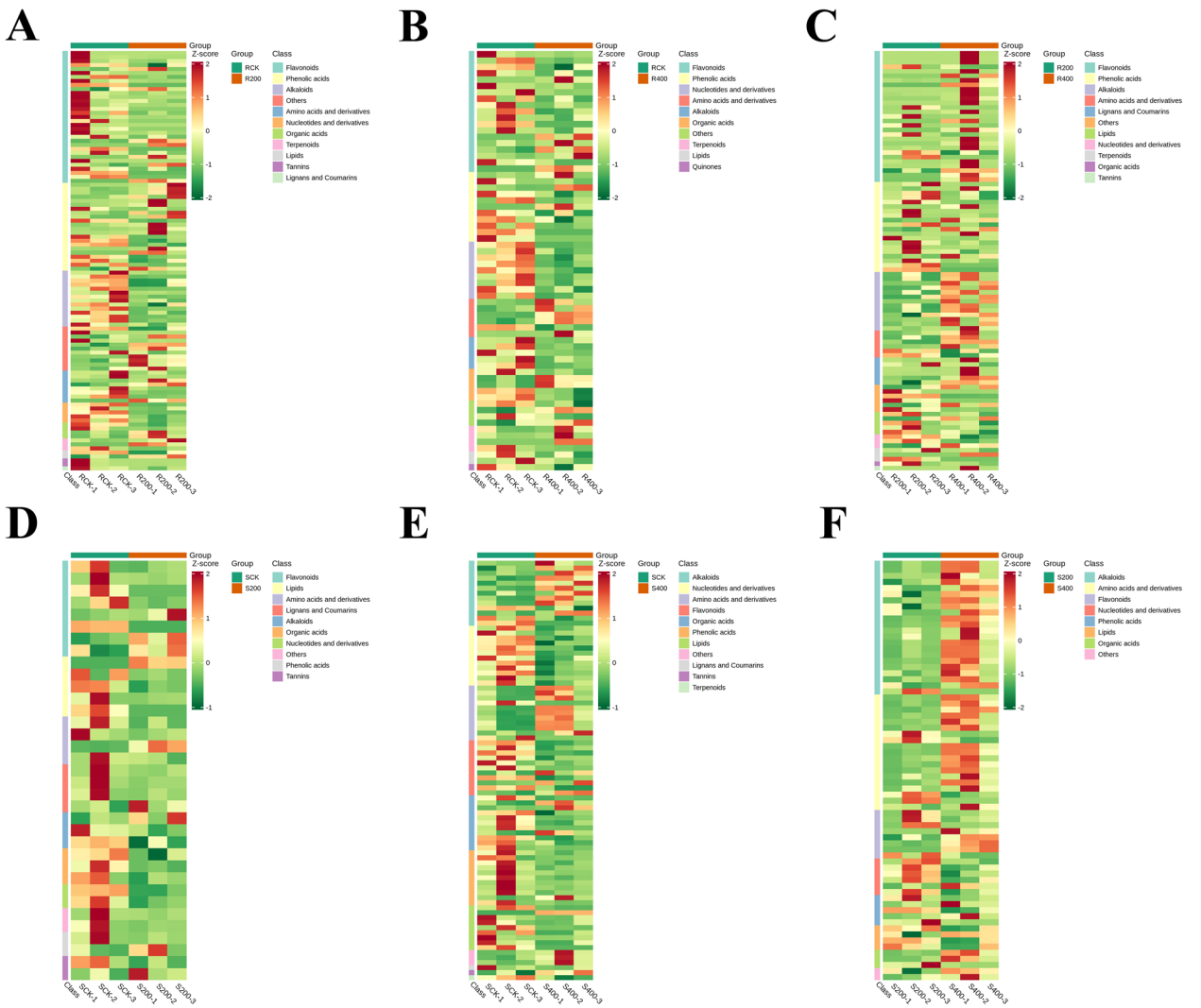

Fig. 8 Heat map of DAMs clustering. **A** RCK_vs_R200. **B** RCK_vs_R400. **C** R200_vs_R400. **D** SCK_vs_S200. **E** SCK_vs_S400. **F** S200_vs_S400

euphratica differed under 200 mM and 400 mM NaCl treatments. However, the majority of the DAMs showed a significant increase after salt treatment. These results suggested that *P. talassica*×*P. euphratica* responded to salt stress by expressing different metabolites (Fig. 9B).

KEGG pathway enrichment analysis of DAMs

To identify the pathways enriched by DAMs, KEGG pathway enrichment analysis was conducted based on the DAMs results. The top 20 pathways were selected and displayed in ascending order of their *P*-values. KEGG pathway enrichment analysis of DAMs was also conducted based on the obtained results of DAMs. Figure 10 shows the KEGG enrichment bubble plots of DAMs of the six comparative groups in the roots and stems of *P. talassica*×*P. euphratica*, revealing significant differences in DAMs among different treatment groups.

In the RCK_vs_R200 comparison group, metabolic pathways such as biosynthesis of secondary metabolites, flavonoid biosynthesis, biosynthesis of cofactors, biosynthesis of amino acids, ABC transporters, and 2-oxocarboxylic acid metabolism were markedly enriched. In the RCK_vs_R400 comparison group, markedly enriched pathways included biosynthesis of secondary metabolites, biosynthesis of amino acids, biosynthesis of cofactors, nucleotide metabolism, ABC transporters, and purine metabolism. In the R200_vs_R400 comparison group, pathways such as biosynthesis of secondary metabolites, flavonoid biosynthesis, phenylpropanoid biosynthesis, flavone and flavonol biosynthesis, tryptophan metabolism, and biosynthesis of amino acids were markedly enriched (Fig. 10).

In the SCK_vs_S200 comparison group, metabolic pathways such as biosynthesis of secondary

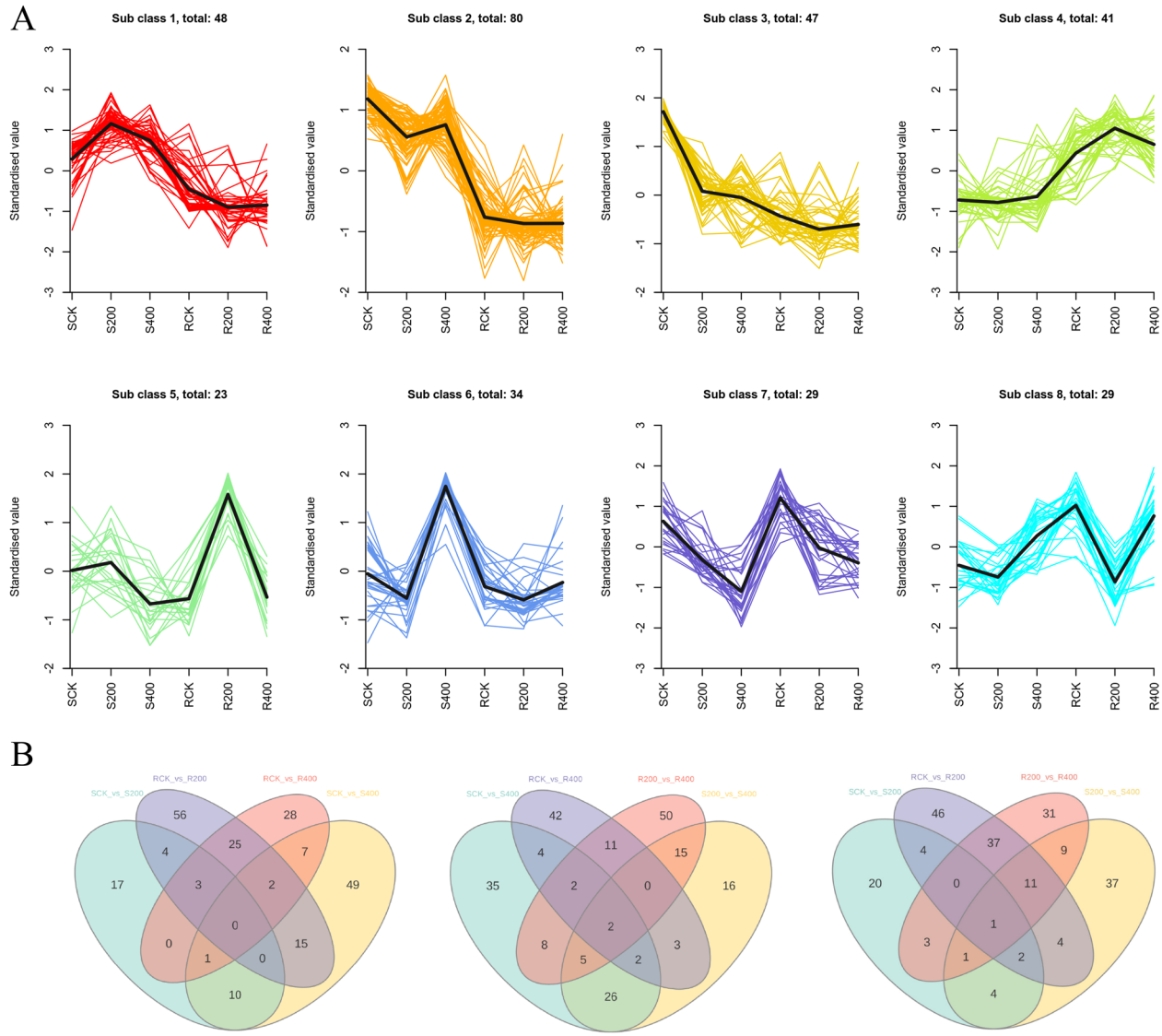

Fig. 9 Clustering and Overlap Analysis of DAMs Across Comparison Groups. **A** K-means clustering analysis charts. **B** Venn diagram of DAMs across comparison groups

metabolites, biosynthesis of various plant secondary metabolites, biosynthesis of cofactors, biosynthesis of amino acids, phenylalanine, tyrosine and tryptophan biosynthesis, and flavonoid biosynthesis were markedly enriched. In the SCK_vs_S400 comparison group, markedly enriched pathways included biosynthesis of secondary metabolites, biosynthesis of amino acids, biosynthesis of cofactors, ABC transporters, purine metabolism, and nucleotide metabolism. In the S200_vs_S400 comparison group, pathways such as biosynthesis of secondary metabolites, biosynthesis of amino acids, biosynthesis of cofactors, ABC transporters, aminoacyl-tRNA biosynthesis, and 2-oxocarboxylic acid metabolism were markedly enriched (Fig. 10).

Transcriptomic metabolomic association analysis

KEGG enrichment bar graph

Bar graphs were generated based on KEGG pathways co-enriched in the two histologies, with the bars representing the number of DAMs and DEGs associated with each pathway. For the amount of shared KEGG pathways exceeding 25, the transcriptomic was used as the basis, and only the pathways with the top 25 *P*-value rankings were displayed. The results are shown in Fig. 11. In the RCK_vs_R200 comparison group, a significant proportion of DEGs and DAMs were enriched in the biosynthesis of amino acids pathway.

Additionally, pathways such as plant hormone signal transduction, carbon metabolism, phenylpropanoid

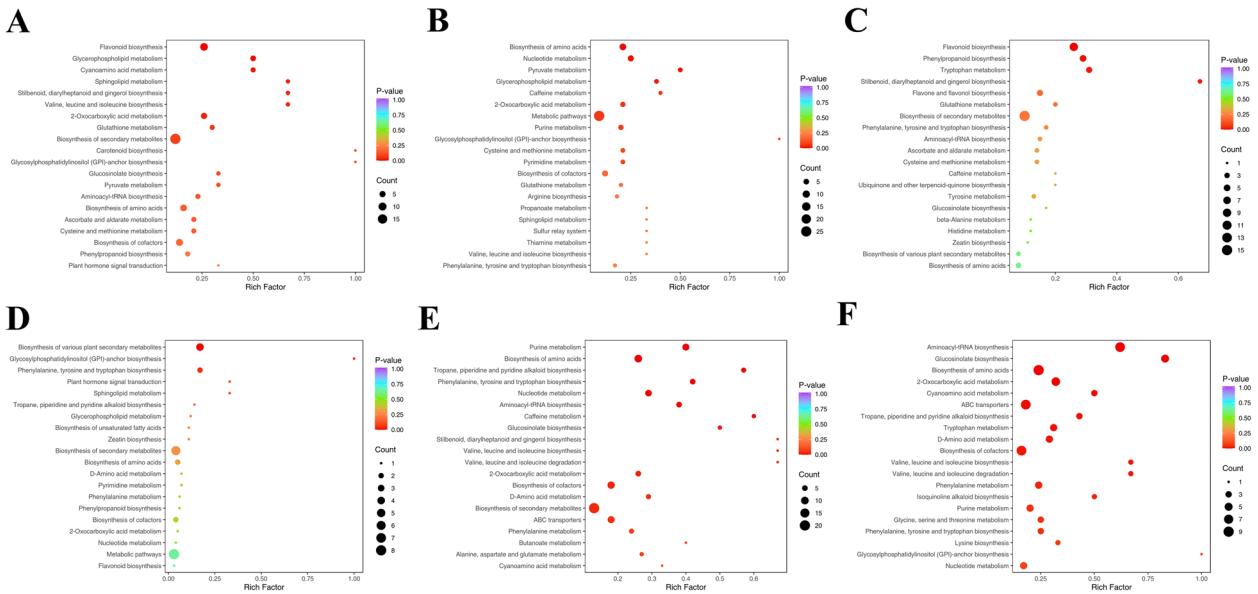

Fig. 10 KEGG enrichment plot of DAMs. **A** RCK_vs_R200. **B** RCK_vs_R400. **C** R200_vs_R400. **D** SCK_vs_S200. **E** SCK_vs_S400. **F** S200_vs_S400

biosynthesis, and starch and sucrose metabolism were notably enriched with DEGs. Similarly, pathways including flavonoid biosynthesis, 2-oxocarboxylic acid metabolism, and ABC transporters exhibited significant enrichment of DAMs. In the RCK_vs_R400 comparison group, a substantial number of DEGs and DAMs were enriched in pathways such as biosynthesis of amino acids and cysteine and methionine metabolism. Additionally, a notable number of DEGs were enriched in the carbon metabolism pathway, while DAMs were markedly enriched in pathways such as purine metabolism, 2-oxocarboxylic acid metabolism, and ABC transporters. In the R200_vs_R400 comparison group, a substantial number of DEGs and DAMs were enriched in pathways such as phenylpropanoid biosynthesis and biosynthesis of amino acids. Additionally, a significant number of DAMs were enriched in the flavonoid biosynthesis pathway (Fig. 11).

In the SCK_vs_S200 comparison group, a substantial number of DEGs and DAMs were enriched in pathways such as biosynthesis of amino acids. Additionally, a notable number of DEGs were enriched in pathways including plant hormone signal transduction, phenylpropanoid biosynthesis, and glycerophospholipid metabolism. In the SCK_vs_S400 comparison group, a significant number of DEGs and DAMs were enriched in the biosynthesis of amino acids pathway. Furthermore, pathways such as carbon metabolism, plant hormone signal transduction, glycolysis/gluconeogenesis, phenylpropanoid biosynthesis, and pyruvate metabolism also exhibited substantial enrichment of DEGs. DAMs were notably enriched in pathways such as purine metabolism and ABC transporters. In the S200_vs_S400 comparison group, a considerable number of DEGs and DAMs were enriched in the biosynthesis of amino acids pathway (Fig. 11). Additionally, a large number of DEGs were enriched in the plant hormone signal transduction pathway, while DAMs were markedly enriched in pathways such as ABC transporters, 2-oxocarboxylic acid metabolism, and phenylalanine metabolism.

In summary, across the comparison groups of roots and stems in *P. talassica*×*P. euphratica*, a substantial number of DEGs and DAMs were enriched in the biosynthesis of amino acids pathway. Additionally, pathways such as plant hormone signal transduction, carbon metabolism, and phenylpropanoid biosynthesis exhibited significant enrichment of DEGs, while pathways including flavonoid biosynthesis, purine metabolism, ABC transporters, and 2-oxocarboxylic acid metabolism showed notable enrichment of DAMs (Fig. 11).

O2PLS analysis

All DEGs and DAMs in the roots and stems of *P. talassica*×*P. euphratica* were selected to plot O2PLS loadings, and the association between DEGs and DAMs was analysed, and the 10 DEGs and DAMs with the strongest associations were screened out, and the results are shown in Fig. 12, and the results are shown in Fig. 12A, which shows that the top 10 DEGs with the strongest influence on metabolomic were *LOC105110065*、*LOC105120036*、*LOC105129277*、*LOC105115394*、*LOC105128125*、*LOC105115927*、*LOC105134725*、*LOC105124002*、*LOC105122358* and *LOC105112769*.

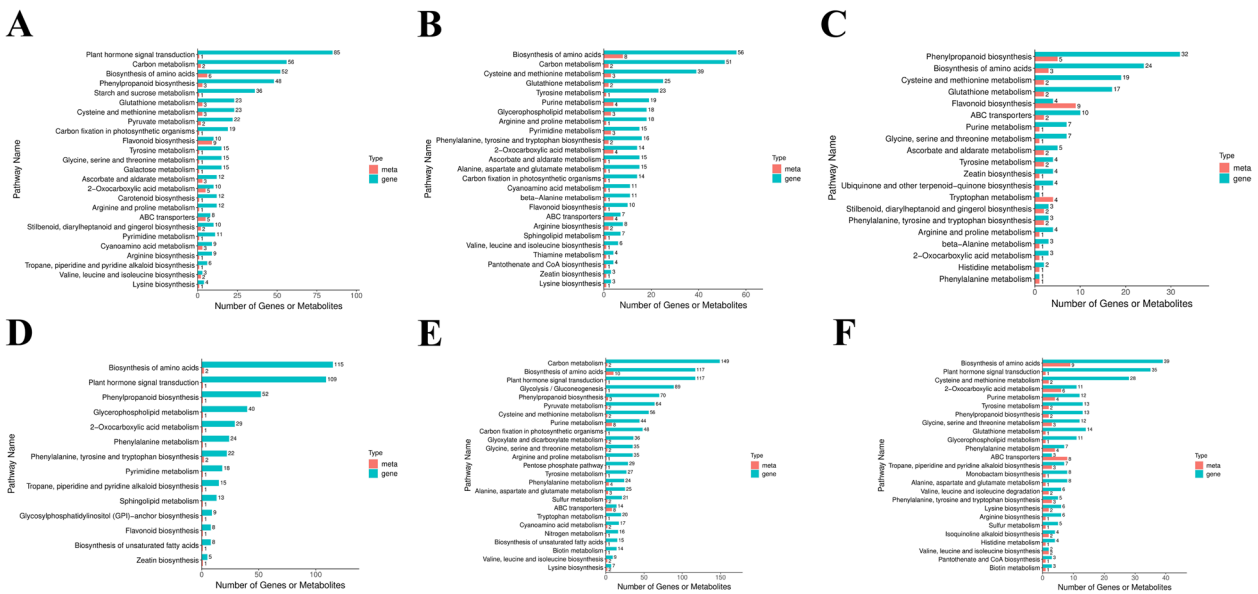

Fig. 11 DEGs and DAMs KEGG enrichment bar graph. **A** RCK_vs_R200. **B** RCK_vs_R400. **C** R200_vs_R400. **D** SCK_vs_S200. **E** SCK_vs_S400. **F** S200_vs_S400

As can be seen in Fig. 12B, the top 10 DAMs with high impact on transcriptomic were Nystose (mws4163), Stachyose (Lmqn000213), Arachidic acid (pmf0397), Xanthosine (mws0668), Uridine 5'-diphosphate (pme3007), Citicoline (MWSmce613), Jasmonoyl-L-Isoleucine (pme2074), Phosphoenolpyruvate (mws2125), Cytidine 5'-monophosphate (Cytidylic acid) (pme3174), Guanosine 3',5'-cyclic monophosphate (mws0609). They were all nucleotides and derivatives, amino acids and derivatives, organic acids, lipids and others class metabolites, which proved that these 10 DEGs and 10 DAMs were closely related to the salt tolerance of *P. talassica* × *P. euphratica*.

Analysis of gene-metabolite interactions in roots and stems of *P. talassica* × *P. euphratica*

Through network analysis, the Fig. 13 reveals the interaction relationship between DEGs that are closely associated with multiple DAMs in the roots and stems of *P. talassica* × *P. euphratica*. From the connections in the Fig. 13, gene *LOC105124002* markedly interacted with multiple DAMs, especially with pme2074. In addition, DEGs *LOC105110065*, *LOC105112988* and *LOC105129286* also interact with multiple DAMs. Gene *LOC105121152* showed significant interactions with both mws1661 and mws0668, while *LOC105134371* also interacted with mws0282 and Lmbn005487 (Fig. 13).

In addition, *LOC105140885*, *LOC105135115*, *LOC105108844*, *LOC105126640*, and *LOC105131256* showed significant interactions with DAMs mws4163, pme0010, pme3033, pme2074, and pme0021, respectively. Among them, *LOC105124002* and *LOC105110065* were among the top 10 DEGs with the most significant impact on metabolomic screened in the O2PLS analysis. *LOC105108844* and *LOC105135115* were DAMs markedly expressed in the roots of *P. talassica* × *P. euphratica*, and *LOC105126640* and *LOC105131256* were DEGs markedly expressed in the stems of *P. talassica* × *P. euphratica*. The DAMs pmb0682, mws0282, Lmbn005487, and pme0021 had significant interactions with several DEGs, which further verified the important roles played by these DEGs and DAMs in the process of salinity resistance of *P. talassica* × *P. euphratica* (Fig. 13).

Accumulation of major metabolites in the biosynthesis of amino acids pathway under salt stress

Under salt stress conditions, upstream and downstream metabolites in the *P. talassica* × *P. euphratica* biosynthesis of amino acids pathway exhibited dynamic regulatory changes, as shown in Fig. 14. Upstream key metabolites such as Shikimate, Anthranilic acid, Phenylpyruvate Phenylpyruvic acidand Phosphoenolpyruvate were markedly downregulated under salt stress. This down-regulation may indicate that precursor resources early in the pathways are reallocated to support the downstream metabolic processes required to combat salt stress (Fig. 14).

In contrast to the upstream metabolites, several downstream metabolites were markedly upregulated, suggesting their critical function in reaction with salt stress. For example, significant accumulation of Histidine, Valine,

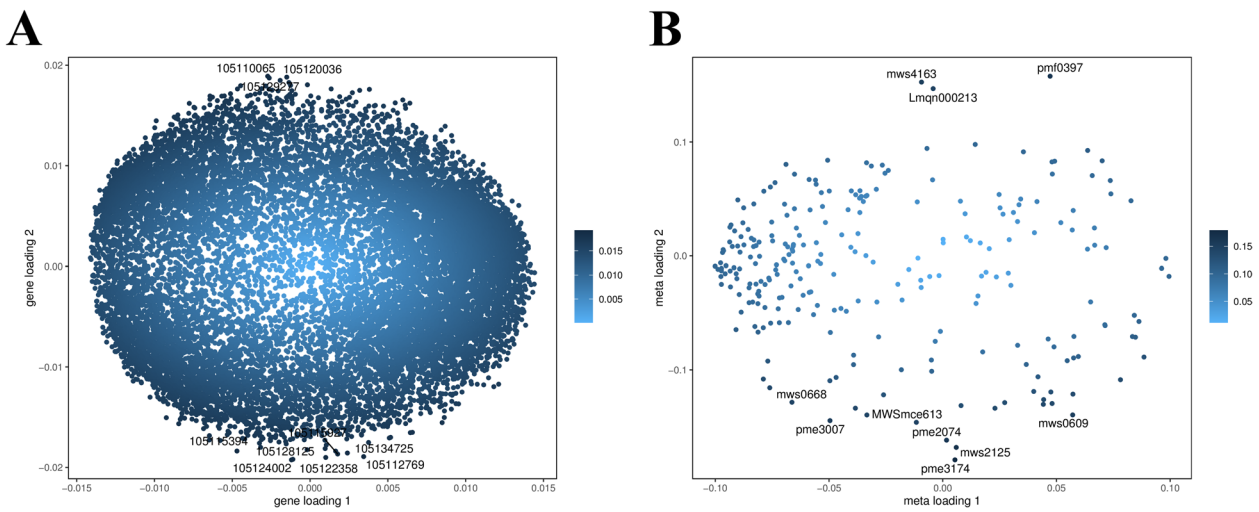

Fig. 12 O2PLS analysis plots. **A** Gene loadings plot. **B** Metabolite loadings plot

Tyrosine, Phenylalanine, Tryptophan and Ornithine indicated their essential function in osmoregulation and antioxidant defence mechanisms. Homoserine, Lysine and N-Acetyl-glutamate were markedly upregulated under 200 mM and 400 mM NaCl treatments were markedly upregulated. These nitrogen-containing metabolites may contribute to the maintenance of cellular homeostasis and the enhancement of salt tolerance by acting as osmolytes or polyamine synthesis precursors. While Glutamine and Asparagine were markedly enriched as key nitrogen transport and storage compounds, reflecting their nitrogen metabolism functions under salt stress conditions (Fig. 14).

Certain metabolites showed specific accumulation patterns under salt stress. For example, 2-Aminoadipate and Serine were markedly downregulated, suggesting their lower metabolic priority in stress acclimation. In contrast, the sustained up-regulation of Leucine and Valine may further play an essential function in salt stress conditions by enhancing protein stability and cellular osmotic homeostasis (Fig. 14).

Discussion

Salt stress is considered one of the most destructive environmental pressures, markedly reducing the productivity and quality of crops worldwide, and severely inhibiting plant growth and development [28]. To enhance crop salt tolerance, it is crucial to clarify the primary plant responses and mechanisms underlying salt tolerance in order to improve crops' ability to tolerate salt stress.

Morphological characteristics and physiological properties

The results of this study showed that 200 mM NaCl treatment promoted the increase of root length, root surface area, count of root tillers, and root-to-shoot ratio of *P. talassica*×*P. euphratica* seedlings to some degree, and resulted in the accumulation of plant biomass. Especially on the second day after the 45th day of NaCl treatment, all the indexes were markedly higher than the control. This results may be related to the ability of saline plants to enhance water and nutrient uptake by regulating the growth of above and below ground parts under low salt stress. It has been reported in the literature that moderate salt stress can stimulate the growth of plant roots and thus improve plant adaptation to salinity [29]. Demonstrating that *P. talassica*×*P. euphratica* is able to improve its growth performance by optimising the root-shoot ratio under low salt stress, this provides strong evidence for the adaptive strategies of saline plants in naturally saline environments.

As the NaCl concentration reached 400 mM, the biomass and root-shoot ratio of *P. talassica*×*P. euphratica* were markedly reduced compared to the control group, with the most pronounced growth inhibition observed on the second day after the 45th day of NaCl treatment. This was attributed to the fact that high concentrations of salt stress usually lead to increased plant water stress and higher osmotic pressure, which inhibit cell expansion and root uptake capacity [30]. This may be the main reason for the decline in biomass of *P. talassica*×*P. euphratica*. More importantly, the decrease in root-shoot ratio further proved that the root growth was limited under high salt stress, and the inability of *P. talassica*×*P. euphratica* to effectively regulate the root-shoot ratio indicated that the threshold of its salt tolerance mechanism had been breached.

In addition, in this study, the RWC change under low salt stress (200 mM NaCl) treatment was small, indicating that the *P. talassica*×*P. euphratica* was able to adapt

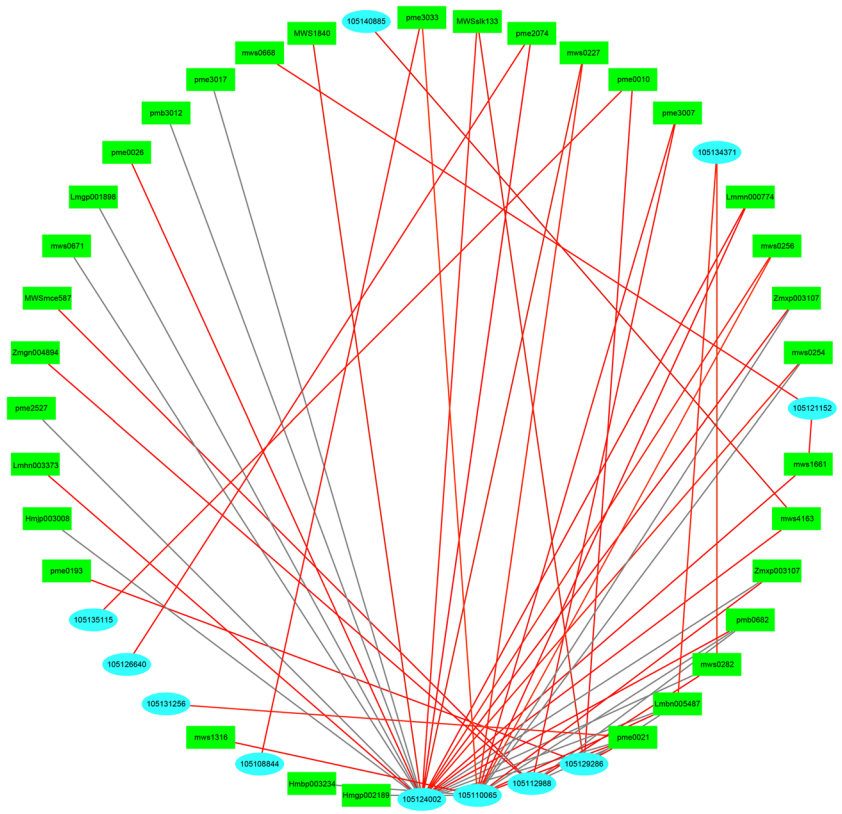

Fig. 13 Gene-metabolite interaction network analysis diagram. Note: The network diagram shown in the figure represents the interactions and relationships between DEGs and DAMs. In the network, each blue box represents a specific gene, each green box represents a metabolite, and the DEGs and DAMs are connected by connecting lines. The lines then represent the interactions between the DEGs and DAMs, with the red lines indicating significant positive correlations or mutually activating relationships, and the grey lines indicating weaker or neutral interrelationships

to low salt concentration, but the water retention capacity of the root system of the *P. talassica*×*P. euphratica* decreased when the NaCl concentration increased to 400 mM. This change reflects, to some extent, the different response mechanisms of *P. talassica*×*P. euphratica* to salt stress. The plant may enhance salt tolerance by altering cellular osmoregulatory substances and root function at low salt concentration, while high salt concentration severely affected the plant's water uptake and retention capacity, resulting in an increased water loss in the plant after salt treatment. This water loss may result from osmotic stress and oxidative stress at high salt concentrations, which in turn triggers intracellular water imbalance and dehydration [31, 32].

In conclusion, the root system of *P. talassica*×*P. euphratica* was able to maintain a high water status under low salt stress, whereas high salt concentration resulted in a significant loss of root water. These results further confirm that under low salt treatment (200 mM NaCl), *P. talassica*×*P. euphratica* is able to coordinate the growth of both aboveground and underground parts, thereby enhancing salt tolerance. This suggests that the 200 mM NaCl treatment may be associated with the plant's ability to tolerate salt through specific physiological mechanisms. In contrast, under high salt concentration (400 mM NaCl), plant growth and water balance are markedly inhibited, which may indicate that this treatment is linked to mechanisms by which the plant reduces salt accumulation or mitigates the damage caused by excessive salt, potentially representing a strategy of salt avoidance.

Transcriptomic analysis

Under high salinity treatment, the number of downregulated DEGs in the roots of *P. talassica*×*P. euphratica* increases, suggesting that gene expression in the roots of *P. talassica*×*P. euphratica* is markedly suppressed as NaCl concentration rises. Moreover, the expression patterns of DEGs in roots and stems showed significant differences under different NaCl treatments. This may be closely related to the mechanisms of salt stress-induced osmoregulation, antioxidant stress response and coping with ion accumulation.

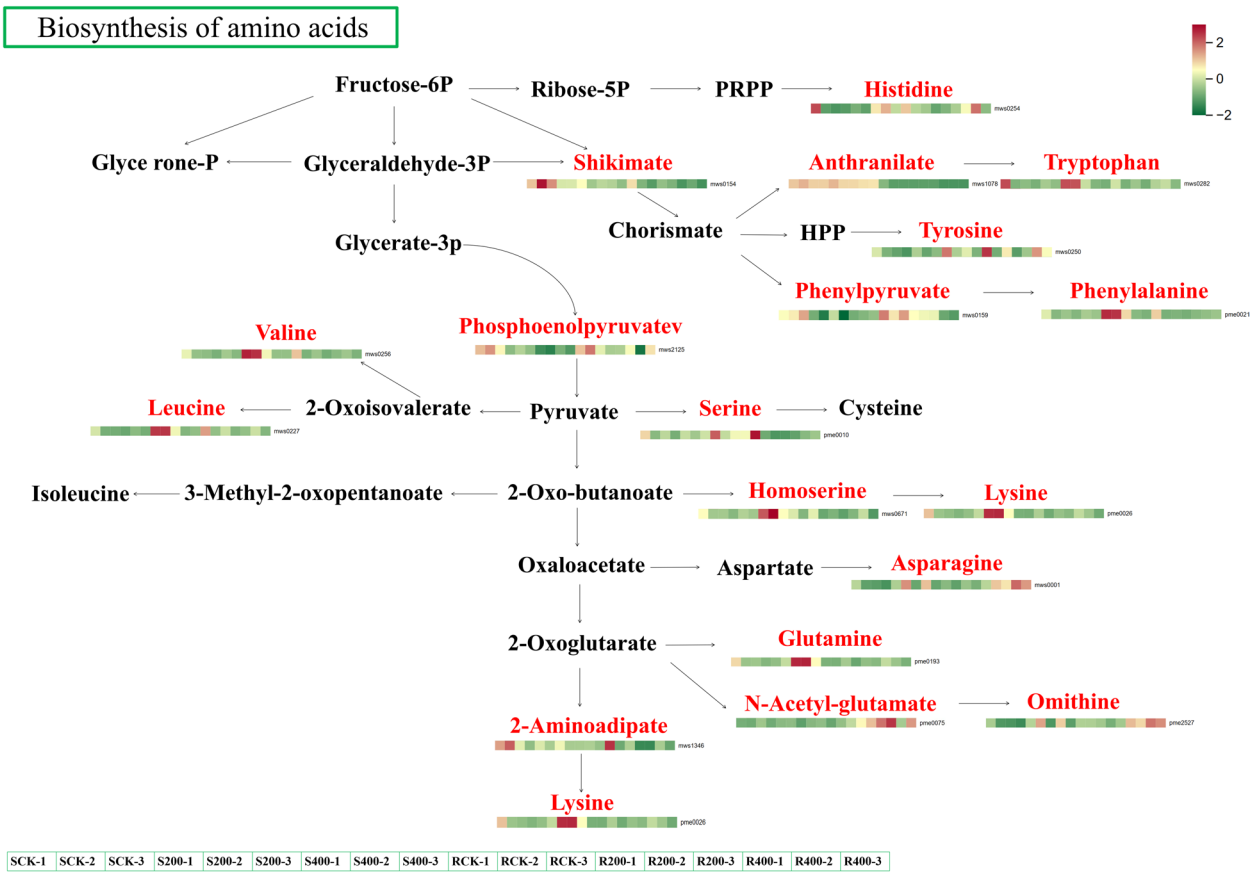

Fig. 14 Heatmap of metabolite changes in biosynthesis of amino acids pathway under NaCl treatment. Note: The boxes in the pathway represent the expression of DAMs, each small square represents one sample. From left to right, the expression of DAMs in samples SCK-1, SCK-2, SCK-3, S200-1, S200-2, S200-3, S400-1, S400-2, S400-3, RCK-1, RCK-2, RCK-3, R200-1, R200-2, R200-3, R400-1, R400-2, R400-3, the redder the colour of the heatmap, the higher the metabolite expression

KEGG pathway enrichment analysis of DEGs following treatment with varying NaCl concentrations

Although significant differences exist in the enrichment of metabolic pathways between the roots and stems, the plant hormone signal transduction pathway is a crucial factor in regulating the salt stress adaptability of *P. talassica*×*P. euphratica*. Plant hormones, particularly ABA and GA, regulate water balance, antioxidant capacity, and growth under salt stress [33, 34].

Screening of key DEGs for salt tolerance

In this study, we compared the DEGs expression patterns in roots and stems of *P. talassica*×*P. euphratica*, with particular attention to the distribution of TFs. The results showed that the markedly DEGs in roots and stems differed in the composition of TFs, which provided new insights into the molecular mechanisms by which plants respond to environmental stimuli in different organs. Firstly, most of the significant DEGs in the stem of *P. talassica*×*P. euphratica* belong to the AP2/ERF, NAC, WRKY, R2R3-MYB, and ocs element-binding factor 1-like TFs. The importance of the AP2/ERF, WRKY, and NAC families of TFs in plant responses to biotic and abiotic stresses has been widely recognised [35–37]. The high expression of AP2/ERF TFs in the stem may be associated with water regulation, promotion of growth and development, and resistance to external stresses in the stem of plants [38]. Meanwhile, the enrichment of R2R3-MYB TFs suggests a key role of stems in phytohormone signalling and cell wall biosynthesis, which may contribute to the maintenance of structural stability of plants under stress [39].

In contrast, the significant DEGs in the roots of *P. talassica*×*P. euphratica* were dominated by AP2/ERF, NAC, bZIP, WRKY, JUNGBRUNNEN 1-like TFs and ocs element-binding factor 1-like families. The high expression of the bZIP TFs in roots indicates its important role in plant root growth, response to water stress and coping with salinity adversity [40]. The bZIP TFs usually help

plant roots to adapt to unfavourable environments by participating in the expression of DEGs regulating light, gas exchange and response to adversity [41]. The DREB TFs in roots also shows high expression, further emphasising its key role in coping with drought and salinity stress [42]. The enrichment of the JUNGBRUNNEN 1-like TFs in roots further implies that *P. talassica*×*P. euphratica* roots may enhance their resistance to salt stress by regulating genes associated with antioxidant responses [43].

The enrichment of the ocs element-binding factor 1-like TFs in roots and stems suggests that *P. talassica*×*P. euphratica* stems may regulate the expression of DEGs involved in the plant antioxidant response and environmental stress response through binding to plant OCS elements, a mechanism that may contribute to stem adaptation under salt stress [44]. These TFs help plants maintain water and nutrient homeostasis in the interroot environment by regulating water metabolism and ion homeostasis.

Taken together, these differences suggest that the expression of TFs in roots and stems of *P. talassica*×*P. euphratica* is highly organ-specific and may be closely related to the physiological functions and adaptive mechanisms of each organ under different environmental conditions. Gene expression patterns in roots may be more focused on responding to water and oxygen stress to safeguard the plant's water and nutrient uptake capacity, while stems may be more effective in reaction with external adversity or mechanical stresses by adjusting growth and development and structural stability [45, 46]. It was demonstrated that the two have different regulatory mechanisms in the genetic response to salt stress.

Metabolomic analysis

Trend analysis of DAMs

In each comparison groups of roots and stems, the number of DAMs differed markedly, indicating that salt stress affected the metabolic network of *P. talassica*×*P. euphratica* to different degrees. Under 200 mM NaCl treatment, the metabolic responses in the roots of *P. talassica*×*P. euphratica* were more active, and the changes in DAMs mainly showed an increase in both upregulated and downregulated DAMs, which might be related to the adaptive mechanism of the roots at the early stage of salt stress. 200 mM NaCl treatment was able to activate the metabolic network of the roots of *P. talassica*×*P. euphratica*, and promote its ability to cope with salt stress. However, as the NaCl concentration was increased to 400 mM, the metabolic response of the roots was markedly weakened and the number of metabolite changes decreased. This may indicate that the osmotic stress and ionic toxicity effects induced with increasing salt concentration resulted in the suppression of metabolic activities in the roots of *P. talassica*×*P. euphratica* [47].

In contrast, metabolic responses in the stem showed a different trend. When the NaCl concentration was increased to 400 mM, the number of DAMs in the stem increased markedly compared with the control, and the number of downregulated DAMs was markedly higher than that of upregulated DAMs. This may be due to the fact that the stem, as the plant's transport and support tissue, has a different adaptation strategy to salt stress than the root, which mainly reduces salt dependence by decreasing the activity of certain metabolic pathways, and thus reduces the physiological stress due to salt stress. Therefore, the metabolic responses triggered by salt stress may act through different mechanisms in roots and stems, thus ensuring plant growth and development under different stress intensities [48].

Dynamic distribution of metabolite differences

The results of the dynamic distribution of metabolite differences revealed different trends of metabolite changes in the roots and stems of *P. talassica*×*P. euphratica* under salt stress, and highlighted the unique metabolic mechanisms in reaction with salt stress. The DAMs that were markedly upregulated in the roots of *P. talassica*×*P. euphratica* included amino acids and derivatives, flavonoids, alkaloids, organic acids and lipids, which may play an essential function in the plant's response to salt stress. The findings align with those previously reported by Guo J et al., in their study on Cotton where they found that under salt stress, cotton can further adapt to osmotic stress through the accumulation of organic acids and amino acids [49]. In analysing the metabolomic of *Nitraria sibirica* Pall. under salt stress, Li H et al. found that the DAMs between salt-free and NaCl treatments were mainly amino acids, organic acids and polyols [50]. In contrast, DAMs that were markedly downregulated in *P. talassica*×*P. euphratica* roots were mainly flavonoids, phenolic acids, nucleotides and derivatives, and terpenoids, and the reduction of these DAMs may be related to the plant's strategy of energy conservation and optimal allocation of resources to cope with the changes in energy and material requirements in high-salt environments.

In the stem, the DAMs that were markedly upregulated were primarily flavonoids, amino acids and derivatives, terpenoids, and organic acid analogues. Flavonoids and terpenoids compounds are integral to the salt resistance mechanism of plants, and these substances have antioxidant and antimicrobial properties, which can effectively reduce the cell damage induced by salt stress. Especially under high salt stress, the accumulation of flavonoids compounds may help to improve the antioxidant capacity

of plants, thus alleviating the negative effects of oxidative stress [51, 52]. In the stem, the DAMs that were markedly downregulated were primarily amino acids and derivatives, lipids and alkaloids, and these changes may be related to the plant's regulation of metabolic priorities in the stem to adjust to the demands of salt stress.

Overall, the metabolic responses of the roots and stems of *P. talassica*×*P. euphratica* showed significant differences under salt stress, and each had unique salt-tolerant metabolites. The salt tolerance mechanism in roots may mainly depend on the accumulation of metabolites such as amino acids and derivatives, flavonoids and alkaloids, which may help plants to cope with salt stress by enhancing osmoregulation, antioxidant capacity, and ion homeostasis regulation. The stem, on the other hand, may enhance its adaptation to salt stress through the accumulation of terpenoids, oganic acids and flavonoids, which are metabolites that not only effectively slow down the impacts of salt stress on plant growth, but also maintain the overall physiological stability of the plant by regulating the cellular metabolism and increasing the antioxidant capacity of the plant.

KEGG pathway enrichment analysis of DAMs

KEGG pathway enrichment analysis showed that *P. talassica*×*P. euphratica* exhibited different metabolic responses under different concentrations of NaCl treatments. The flavonoid biosynthesis pathway was markedly enriched in both roots and stems under 200 mM NaCl treatment, suggesting an important salt tolerance role under salt stress [53]. In contrast, nucleotide metabolism [54] and purine metabolism [55] pathways were markedly enriched under 400 mM NaCl treatment, suggesting that plants respond to salt stress by regulating nucleotide metabolic pathways at higher salt concentrations.

This result suggests that *P. talassica*×*P. euphratica* adopted different metabolic strategies under different salt concentrations, responding mainly through secondary metabolite synthesis under moderate salt stress and shifting to nucleotide metabolism-related pathways under high salt stress. In addition, although roots and stems are co-enriched in biosynthesis of secondary metabolites, biosynthesis of cofactors, biosynthesis of amino acids, flavonoid biosynthesis, and ABC transporters and other metabolic pathways, there are some differences.

Root-specific enrichment pathways include phenylpropanoid biosynthesis, flavone and flavonol biosynthesis, and tryptophan metabolism, which are closely related to plant resistance and stress response [56–58]. In contrast, stems were enriched for biosynthesis of various plant secondary metabolites, phenylalanine, tyrosine and tryptophan biosynthesis, and aminoacyl-tRNA biosynthesis metabolic pathways, suggesting that stems maintain cellular integrity and protein synthesis through extensive metabolic adjustments [59–61]. These results are consistent with other studies on salt-tolerant plants, suggesting that plants respond to salt stress through specific metabolic regulation at different parts [62]. Differences in metabolic pathways enriched in roots and stems further emphasise the importance of tissue-specific adaptation in plant response to salt stress (Fig. 15).

Transcriptomic and metabolomic integration analysis

Transcriptomic and metabolomic have opened new avenues for discovering genes related to plant adaptation to stress, identifying gene functions, and detecting secondary metabolites [63]. Based on the combined transcriptomic and metabolomic analysis, the study identified alterations in multiple metabolic pathways in reaction with salt stress in the roots and stems of *P. talassica*×*P. euphratica*.

Notably, the biosynthesis of amino acids pathway showed the highest enrichment of DEGs and DAMs in all comparison groups of roots and stems, indicating the prominent regulatory role of amino acid metabolism under salt stress. In addition, several key metabolic pathways such as plant hormone signal transduction, carbon metabolism and phenylpropanoid biosynthesis showed significant in DEGs enrichment, while flavonoid biosynthesis, purine metabolism, ABC transporters and 2-Oxocarboxylic acid metabolism were significant in DAMs enrichment analysis.

Amino acid metabolism pathway plays an essential function in protein biosynthesis, is an integral part of several biosynthetic pathways, and is involved in signal transduction processes during plant response to adversity [64]. This study found significant enrichment in the biosynthesis of amino acids pathway, suggesting that NaCl alleviates damage to *P. talassica*×*P. euphratica* by regulating amino acid metabolism. It also highlights the close relationship between amino acid metabolism and salt stress, emphasizing its essential function in reaction with salt stress.

In addition, phytohormones usually require complex signalling networks in combination with other signalling pathways to perform their normal functions. Therefore, understanding plant hormone signalling is a prerequisite for studying plant defence mechanisms against adversity [65]. Similar to our study, Wang GL et al. found that the identified DEGs were primarily involved in pathways such as plant hormone signal transduction and MAPK signaling pathway-plant, which have been widely reported in other plant species [66]. Research on *Clerodendrum inerme* [67], *Sophora alopecuroides* [68], Cotton [69], and *Aquilegia* [70] has shown significant changes in

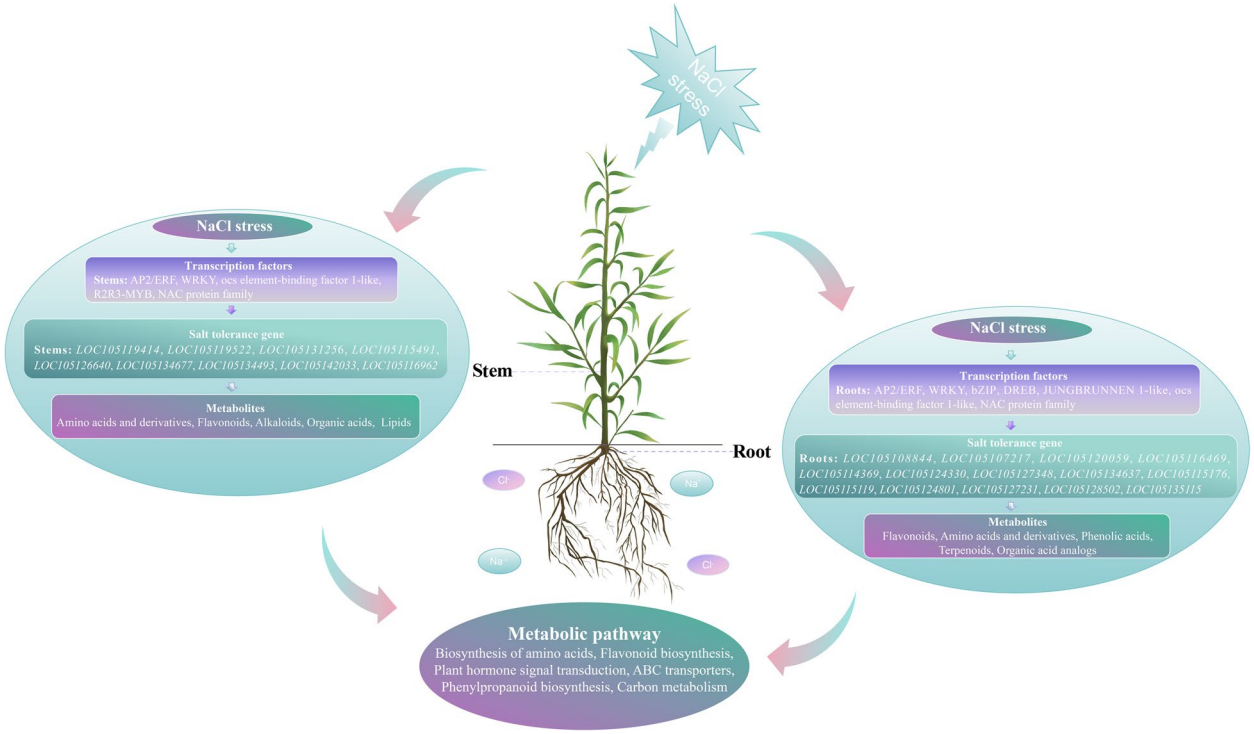

Fig. 15 DEGs, DAMs and pathways for salt tolerance of *P. talassica*×*P. euphratica*

genes associated with the plant hormone signal transduction pathway under salt stress conditions. Significant alterations were observed in the genes associated with the plant hormone signal transduction pathway, and the DEGs were mainly annotated in the plant hormone signal transduction pathway, which proved that the plant hormone signal transduction pathway contribute markedly to the growth process of crops.

Extensive research has demonstrated that metabolic pathways such as carbon metabolism [71, 72], phenylpropanoid biosynthesis [56], flavonoid biosynthesis [73], purine metabolism [74], ABC transporters [75], and 2-oxocarboxylic acid metabolism [76] are closely associated with plant salt tolerance, indicating their essential function in the response of *P. talassica*×*P. euphratica* to salt stress. Through the aforementioned pathways, *P. talassica*×*P. euphratica* gradually adapts to salt stress, alleviating cell damage caused by osmotic stress, energy metabolism disturbances, and oxidative stress.

Under continuous salt stress, *P. talassica*×*P. euphratica* enhances secondary metabolic pathways, such as the synthesis of flavonoids and phenylpropanoids. These compounds not only possess antioxidant properties but also contribute markedly to the structural fortification of *P. talassica*×*P. euphratica* tissues, thereby enhancing its long-term adaptability to environmental stressors [77].

O2PLS analysis and gene-metabolite interaction network analysis

O2PLS analysis revealed strong associations between DEGs and DAMs in *P. talassica*×*P. euphratica* roots and stems. The top 10 DEGs with the most significant impact on metabolomic, including *LOC105110065* and *LOC105124002*, showed significant associations with multiple metabolites suggesting that they may play an important role in the regulation of salt tolerance. The top 10 DAMs with high impact on transcriptomic, such as Nystose (mws4163), Xanthosine (mws0668), and Jasmonoyl-L-Isoleucine (pme2074), are involved in nucleotides and derivatives, amino acids and derivatives, organic acids and lipids. These metabolites are not only closely related to the salt tolerance of *P. talassica*×*P. euphratica*, but also may enhance its salt tolerance by regulating the response mechanism of plant cells.

In addition, the results suggest that the molecular mechanism of salt tolerance in *P. talassica*×*P. euphratica* may involve the coordinated regulation of multiple metabolic pathways. In particular, the interaction between DEGs such as *LOC105124002* and specific metabolites, such as Jasmonoyl-L-Isoleucine (pme2074), suggests that the salt stress response of plants may be regulated through the modulation of phytohormone synthesis and signal transduction. Jasmonic acid and its derivatives play an important role in plant stress tolerance,

and it has been shown that jasmonic acid can improve salt stress tolerance by regulating the activity of antioxidant enzymes and enhancing plant membrane stability [78]. Thus, the strong association of *LOC105124002* with Jasmonoyl-L-Isoleucine (pme2074) may reveal an important regulatory pathway for salt tolerance. Other gene-metabolite interactions also provide new insights into the mechanism of salt tolerance in *P. talassica*×*P. euphratica*, suggesting that mutual regulation between DEGs and metabolites may act synergistically under salt stress.

Accumulation of major metabolites in the biosynthesis of amino acids pathway in *P. talassica*×*P. euphratica* under salt stress

Under salt stress conditions, the biosynthesis of amino acids pathway in *P. talassica*×*P. euphratica* exhibits significant metabolic remodeling. The substantial down-regulation of upstream metabolites, including Shikimate, Anthranilic acid, Phenylpyruvic acid, and Phosphoenolpyruvate, suggests that plants may suppress the accumulation of these early precursors to prioritize the allocation of metabolic resources to downstream products with greater stress-adaptive functions. This reallocation of metabolic flux aligns with the strategy of efficient energy and resource utilization and may also help plants maintain a balance between carbon and nitrogen metabolism under salt stress [79].

The reduction in Phosphoenolpyruvate may be associated with its competitive demand in glycolysis and the TCA cycle, thereby facilitating the biosynthesis of amino acids and other secondary metabolites [80]. The significant up-regulation of downstream metabolites highlights their essential function under salt stress. For instance, the notable accumulation of Histidine, Valine, Tyrosine, Phenylalanine, and Tryptophan indicates that these metabolites not only contribute to protein synthesis but also are essential for osmotic regulation and antioxidant defense [81, 82]. Previous studies have demonstrated that aromatic amino acids, such as Phenylalanine and Tryptophan, serve as precursors for secondary metabolites (phenolic compounds and indole derivatives), which are critical in mitigating the accumulation of reactive oxygen species [83, 84].

The up-regulation of Ornithine may enhance membrane stability and alleviate oxidative damage by promoting the synthesis of polyamines, such as spermidine and spermine [85]. Among nitrogen-containing metabolites, the significant up-regulation of Homoserine, Lysine, and N-Acetyl-glutamate further indicates that salt stress induces a redistribution of nitrogen metabolism to maintain cellular homeostasis. For instance, N-Acetyl-glutamate, as a precursor for Ornithine and polyamine synthesis, is likely to play an essential function in the salt tolerance mechanisms of plants [86, 87]. Furthermore, the enrichment of Glutamine and Asparagine not only reflects their essential function as nitrogen storage and transport molecules but also highlights their involvement in regulating cellular nitrogen balance and amino acid cycling under salt stress, thereby enhancing the adaptive capacity of plants [88, 89].

In addition, differences in metabolite accumulation patterns provide valuable insights into metabolic priorities. For example, the down-regulation of 2-Aminoadipate and Serine may indicate that they play a less significant role in stress response, while metabolic resources being preferentially allocated to other key metabolites [90]. In contrast, the sustained up-regulation of Leucine and Valine may further support plant survival in high-salt environments by enhancing protein stability and regulating intracellular osmotic pressure [91, 92].

Taken together, the dynamic changes of these metabolites demonstrated the precise mechanisms of energy and substance regulation in *P. talassica*×*P. euphratica* under salt stress. On the one hand, the reduction of upstream metabolites reflects the redistribution of metabolic flux to ensure the synthesis of downstream key metabolites. On the other hand, the significant accumulation of downstream metabolites highlighted their physiological roles in salt stress resistance. These metabolic regulatory strategies suggest that *P. talassica*×*P. euphratica* effectively coordinates carbon and nitrogen balance and enhances stress tolerance mechanisms through reprogramming metabolic networks to adapt to salt stress.

Similar to our study, Wu Y et al. reported in their research on *Carex rigescens* that six amino acids involved in the amino acid biosynthesis pathway—namely, Valine, Phenylalanine, Isoleucine, Tryptophan, Threonine, and Serine were accumulated following salt stress treatment [93]. Likewise, Hildebrandt TM et al. observed in Arabidopsis that several highly abundant amino acids, including proline, arginine, asparagine, glutamine, and GABA, are synthesized during abiotic stress. These amino acids function as compatible osmolytes, precursors for secondary metabolites, or storage forms of organic nitrogen [94]. It has been demonstrated that these amino acid analogues are also crucial for the stress resistance of *P. talassica*×*P. euphratica*.

Conclusions

This study first reveals the growth and physiological response patterns of *P. talassica*×*P. euphratica* seedlings under salt stress. The 200 mM NaCl treatment markedly increased root length, root surface area, root branching number, and root-to-shoot ratio, and contributed to the accumulation of plant biomass. Particularly on the second day after the 45th day of NaCl treatment, all morphological parameters were markedly higher than those

in the control group. Under moderate low salt stress, *P. talassica*×*P. euphratica* is able to coordinate the growth of both aboveground and underground parts, enhancing salt tolerance. This suggests that under low salt conditions, *P. talassica*×*P. euphratica* may exhibit salt tolerance. However, under 400 mM NaCl treatment, biomass accumulation, root length, root surface area, root branching number, root-to-shoot ratio, and RWC were all markedly lower compared to the control, with the most pronounced effects observed on the second day after the 45th day of NaCl treatment. This suggests that high-concentration salt stress inhibits the growth and water balance of *P. talassica*×*P. euphratica*.

The above results further proved that under the low salt treatment (200 mM NaCl), *P. talassica*×*P. euphratica* was able to coordinate the growth of above-ground and below-ground parts and enhance the salt tolerance, which indicated that the salt treatment might be associated with the plant's ability to tolerate salinity through certain physiological mechanisms. Whereas, under high salt concentration (400 mM NaCl), the growth and water balance of the plant were markedly inhibited, which may indicate that the treatment is associated with the plant's ability to reduce salt accumulation or control salt-induced damage through certain mechanisms, and may be a strategy for the plant to avoid salt.

Meanwhile, transcriptomic analysis revealed that the pathways involved in gene enrichment in roots and stems of *P. talassica*×*P. euphratica* differed in the salt tolerance response, suggesting that roots and stems may adapt to salt stress through different metabolic mechanisms. In addition, several core pathways such as plant hormone signal transduction、phenylpropanoid biosynthesis、MAPK signaling pathway−plant、plant−pathogen interaction、glycolysis / gluconeogenesis、carbon metabolism、biosynthesis of amino acids、ABC transporters、pyruvate metabolism, and several key TFs such as AP2/ERF, NAC, WRKY and bZIP [22].

The results showed that the DAMs that were markedly upregulated in both roots and stems of *P. talassica*×*P. euphratica* were mainly flavonoids, amino acids and derivatives, of which the upregulated DAMs specific to stems included alkaloids, organic acids and lipids, while the upregulated DAMs specific to roots were phenolic acids, terpenoids and organic acid analogs. The DAMs that were markedly downregulated in both roots and stems were mainly flavonoids, phenolic acids, nucleotides and derivatives, while the downregulated DAMs specific to stems included amino acids and derivatives, lipids and alkaloids in stems, and terpenoids in roots.These results suggest that unique salt-tolerant metabolites are present in both roots and stems of *P. talassica*×*P. euphratica* in reaction with external salt stress.

KEGG pathway enrichment analysis showed that flavonoid biosynthesis pathway was the unique salt-tolerant metabolic pathway in the roots and stems of *P. talassica*×*P. euphratica* under 200 mM NaCl treatment, whereas nucleotide metabolism and purine metabolism metabolic pathways were the metabolic pathways in the roots of *P. talassica*×*P. euphratica* under 400 mM NaCl treatment. This is a unique salt-tolerant pathway in the roots and stems of *P. talassica*×*P. euphratica*, which is a unique salt-tolerant way in reaction with different concentrations of salt stress. In addition, the metabolic pathways of biosynthesis of secondary metabolites, biosynthesis of cofactors, biosynthesis of amino acids, flavonoid biosynthesis, and ABC transporters were jointly enriched in the roots and stems of *P. talassica*×*P. euphratica*.

The unique metabolic pathways enriched in roots were phenylpropanoid biosynthesis, flavone and flavonol biosynthesis, and tryptophan metabolism pathway. The unique metabolic pathways enriched in stems were the biosynthesis of various plant secondary metabolites, phenylalanine, tyrosine and tryptophan biosynthesis, and aminoacyl-tRNA biosynthesis pathways, demonstrating that the metabolic pathways enriched in roots and stems of *P. talassica*×*P. euphratica* are somewhat different in reaction with salt stress.

Finally, through transcriptomic and metabolomic integrated analysis, the metabolic regulation characteristics of *P. talassica*×*P. euphratica* under different salt stress conditions were revealed. KEGG enrichment analysis showed that the biosynthesis of amino acids pathway was markedly enriched in all comparison groups. Both in the roots and stems of *P. talassica*×*P. euphratica*, a large number of DEGs and DAMs were enriched, indicating the central role of this pathway in the plant's response to salt stress. In addition, several important pathways, such as plant hormone signal transduction, carbon metabolism, and phenylpropanoid biosynthesis, also exhibited significant enrichment of DEGs in various comparison groups, highlighting the critical roles of these pathways in the salt stress response.

Furthermore, the enrichment of DEGs in pathways such as flavonoid biosynthesis, purine metabolism, ABC transporters, and 2-oxocarboxylic acid metabolism was also observed in specific groups, particularly in the RCK_vs_R400 and SCK_vs_S400 comparison groups. This suggests that these DAMs may contribute to salt tolerance in plants by regulating cellular osmotic pressure and enhancing antioxidant capacity under high salt stress conditions.

The associations between DEGs and DAMs in roots and stems of *P. talassica*×*P. euphratica* were revealed by O2PLS analysis. The top 10 DEGs with

the most significant impact on metabolomic were *LOC105110065* and *LOC105124002*, among others, whereas the top 10 DAMs with high impact on transcriptomic included Nystose (mws4163), Xanthosine (mws0668) and Jasmonoyl-L- Isoleucine (pme2074).

These DEGs and DAMs were mainly involved in nucleotides and derivatives, amino acids and derivatives, organic acids and lipids, suggesting that they were closely related to the salt tolerance of *P. talassica*×*P. euphratica*. Interaction network analysis further revealed significant interactions between these DEGs and several DAMs, especially the strong association between gene *LOC105124002* and metabolites such as Jasmonoyl-L-Isoleucine (pme2074), verifying their important roles in the mechanism of salt tolerance of *P. talassica*×*P. euphratica*.

In summary, using transcriptomic and metabolomic datasets, this study successfully identified many candidate DEGs and DAMs that are involved in the key biological pathways behind salt tolerance in *P. talassica*×*P. euphratica*. For example, the key role of biosynthesis of amino acids and plant hormone signal transduction in reaction with salt stress in *P. talassica*×*P. euphratica* cannot be ignored. And the interactions between DEGs and DAMs play an important role in salt stress resistance in *Populus tremula*. These findings enhance our understanding of the transcriptional and metabolic mechanisms of salt tolerance in *P. talassica*×*P. euphratica*, offer new perspectives for further research on the salt tolerance mechanisms of this species, and lay a foundation for the future improvement of salt tolerance in *Populus* plants.

Abbreviations

DEGs	Differentially expressed genes
TFs	Transcription factors
FC	Fold change
PCA	Principal component analysis
MS	Mass Spectrometry
DAMs	Differentially accumulated metabolites
UPLC	Ultra Performance Liquid Chromatography
RWC	Relative water content

Supplementary Information

The online version contains supplementary material available at https://doi.org/10.1186/s12870-025-06288-1.

Supplementary Material 1.

Acknowledgements

We thank International Science Editing (http://www.internationalscienceediting.com) for editing this manuscript.

Authors' contributions

Y.L. designed the study, executed the experiment, collected and analyzed data, and wrote the first draft. Z.J.H. oversaw the study, led the experimental design, guided data analysis, and critically reviewed the technical content and structure. Z.Y.L. optimized the research protocol, supervised data analysis, and revised the results and discussion sections. M.X.S. assisted with experimental materials, participated in the experiment, and helped revise the paper. X.Q.Z. and M.L.L. contributed to data collection, organization, and provided equipment and technical support. J.J.W. and X.F.W. processed data, performed statistical analyses, and assisted with graph production. All authors reviewed and approved the final manuscript.

Funding

This work was funded by the open project of State Key Laboratory Incubation Base for Conservation and Utilization of Bio-Resource in Tarim Basin (Funding number: BRZD1902, Funder: Corps Key Laboratory). This work was also funded by the Selection and Cultivation Project of "Talents of Xinjiang Production and Construction Corps" (Funding number: 38000020924, Funder: Xinjiang Production and Construction Corps. Inner Mongolia"Grassland Talents"Leading Talents Programme (2023.01 - 2027.12).

Data availability

The RNA-seq datasets from 27 root, stem and leaf samples of *P. talassica* × *P. euphratica* were uploaded at the NCBI Sequence Read Archive (SRA) database; PRJNA819946: The hybrid of *Populus talassica* and *P. euphratica* Transcriptomic. (TaxID:2,929,483); Reviewer link: https://submit.ncbi.nlm.nih.gov/subs/

Declarations

Ethics approval and consent to participate

All plant-related procedures complied with the relevant institutional, national, and international guidelines and legislation. Consent for publication Not applicable.

Competing interests

The authors declare no competing interests.

Author details

[1]College of Life Science and Technology, Tarim University, State Key Laboratory Incubation Base for Conservation and Utilization of Bio-Resource in Tarim Basin, Alar 843300, China. [2]School of Life Science, Inner Mongolia University, Hohhot 010020, China. [3]Inner Mongolia Academy of Agricultural and Animal Husbandry Sciences, Hohhot 010031, China.

Received: 18 October 2024 Accepted: 21 February 2025
Published online: 20 March 2025

References

1. Hassani A, Azapagic A, Shokri N. Global predictions of primary soil salinization under changing climate in the 21st century. Nat Commun. 2021;12(1):6663.
2. Sun WJ, Jiang XH, Fu YY, et al. The effects of salt stress on chlorophyll fluorescence of cotton seedling leaves. J Irrig Drain. 2021;40:23–8.
3. Lin E, Liu H, Li X, et al. Promoting the production of salinized cotton fifield by optimizing water and nitrogen use effificiency under drip irrigation. J Arid Land. 2021;13:699–716.
4. Wang R, Kang Y, Wan S, et al. Salt distribution and the growth of cotton under different drip irrigation regimes in a saline area. Agric Water Manag. 2011;100(1):58–69.
5. Chen W, Hou Z, Wu L, et al. Evaluating salinity distribution in soil irrigated with saline water in arid regions of northwest China. Agric Water Manag. 2010;97(12):2001–8.
6. Wang W, Wu Z, He Y, et al. Plant growth promotion and alleviation of salinity stress in *Capsicum annuum* L. by Bacillus isolated from saline soil in Xinjiang. Ecotoxicol Environ Saf. 2018;164:520–9.
7. Che J, Zhu YL, Li YH, et al. Response of bacterial communities in saline-alkali soil to different pesticide stresses. Environ Sci Pollut Res. 2022;29(28):42709–19.
8. Xi JB, Zhang FS, Mao DR, et al. Saline-soil distribution and halophyte resources in Xinjiang. Chin J Soil Sci. 2005;36(3):299–303.
9. Munns R, Tester M. Mechanisms of salinity tolerance. Annu Rev Plant Biol. 2008;59(1):651–81.
10. Qin X, Yin Y, Zhao J, et al. Metabolomic and transcriptomic analysis of *Lycium chinese* and *L. ruthenicum* under salinity stress. BMC Plant Biol. 2022;22(1):1–18.

11. Meng N, Yu BJ, Guo JS. Ameliorative efects of inoculation with Bradyrhizobium japonicum on *Glycine max* and *Glycine soja* seedlings under salt stress. Plant Growth Regul. 2016;80(2):137–47.
12. Horie T, Karahara I, Katsuhara M. Salinity tolerance mechanisms in glycophytes: an overview with the central focus on rice plants. Rice. 2012;5(1):1–18.
13. Li H, Duijts K, Pasini C, et al. Effective root responses to salinity stress include maintained cell expansion and carbon allocation. New Phytol. 2023;238(5):1942–56.
14. Flowers TJ, Colmer TD. Salinity tolerance in halophytes. New Phytol. 2008;179(4):945–63.
15. Ba Yanlei. Research on *P. euphratica* cross-breeding and demonstration of new varieties. Xinjiang Uygur Autonomous Region: Xinjiang Academy of Forestry Sciences (Chinese); 2010.
16. BA Yanlei, CUI Peiyi, ZHANG Dongya, et al. Preliminary report on the selection of *P. talassica* × *P. euphratica* hybrid and salt resistance test[C]//The Forest Genetic Breeding Branch of the Society of Forestry of China. Proceedings of the Sixth National Conference on Forest Tree Genetic Breeding. Xinjiang Jimushar Forest Tree Breeding Experiment Station: Xinjiang Academy of Forestry Sciences (Chinese); 2008. p. 1.
17. Sun Yang. Preliminary study on the physiological and ecological resistance of *P. talassica* × *P. euphratica* [D]. Tarim University (Chinese); 2021.
18. Fu Chao. *P. talassica* × *P. euphratica* 'son inherited his father's business' to devote to desert management[N]. Xinjiang Science and Technology News (Chinese); 2010.
19. Zhang M, Xing Y, Ma J, et al. Investigation of the response of *Platycodongrandiflorus* (Jacq.) A. DC to salt stress using combined transcriptomics and metabolomics. BMC Plant Biol. 2023;23(1):589.
20. Han M, Cui R, Wang D, et al. Combined transcriptomic and metabolomic analyses elucidate key salt-responsive biomarkers to regulate salt tolerance in cotton. BMC Plant Biol. 2023;23(1):245.
21. Lu X, Chen G, Ma L, et al. Integrated transcriptome and metabolome analysis reveals antioxidant machinery in grapevine exposed to salt and alkali stress. Physiol Plant. 2023;175(3):e13950.
22. Liu Y, Han ZJ, Su MX, et al. Transcriptomic profile analysis of *Populus talassica* × *Populus euphratica* response and tolerance under salt stress conditions. Genes (Basel). 2022;13(6):1032.
23. Beritognolo I, Piazzai M, Benucci S, et al. Functional characterisation of three Italian *Populus alba* L. genotypes under salinity stress. Trees. 2007;21:465–77.
24. Sade N, Galkin E, Moshelion M. Measuring Arabidopsis, tomato and barley leaf relative water content (RWC). Bio-protocol. 2015;5(8):e1451.
25. Ogata H, Goto S, Sato K, et al. KEGG: kyoto Encyclopedia of Genes and Genomes. Nucleic Acids Res. 1999;27(1):29–34.
26. Chong J, Xia J. MetaboAnalystR: an R package for flexible and reproducible analysis of metabolomics data. Bioinformatics. 2018;34(24):4313–4.
27. Kind T, Wohlgemuth G, Lee DY, et al. FiehnLib: mass spectral and retention index libraries for metabolomics based on quadrupole and time-of-flight gas chromatography/mass spectrometry. Anal Chem. 2009;81(24):10038–48.
28. Zhao S, Zhang Q, Liu M, et al. Regulation of plant responses to salt stress. Int J Mol Sci. 2021;22(9):4609.
29. Hasegawa PM, Bressan RA, Zhu JK, et al. Plant cellular and molecular responses to high salinity. Annu Rev Plant Biol. 2000;51(1):463–99.
30. Chaves MM, Oliveira MM. Mechanisms underlying plant resilience to water deficits: prospects for water-saving agriculture. J Exp Bot. 2004;55(407):2365–84.
31. Parida AK, Das AB. Salt tolerance and salinity effects on plants: a review. Ecotoxicol Environ Saf. 2005;60(3):324–49.
32. Munns R, James RA, Läuchli A. Approaches to increasing the salt tolerance of wheat and other cereals. J Exp Bot. 2006;57(5):1025–43.
33. Jiang W, Wang X, Wang Y, et al. S-ABA enhances rice salt tolerance by regulating Na^+/K^+ balance and hormone homeostasis. Metabolites. 2024;14(4):181.
34. Yu C, Zhou F, Wang R, et al. B2, an abscisic acid mimic, improves salinity tolerance in winter wheat seedlings via improving activity of antioxidant enzymes. Front Plant Sci. 2022;13:916287.
35. Zhang G, Chen M, Li L, et al. Overexpression of the soybean *GmERF3* gene, an AP2/ERF type transcription factor for increased tolerances to salt, drought, and diseases in transgenic tobacco. J Exp Bot. 2009;60(13):3781–96.
36. Liang Q, Wu Y, Wang K, et al. Chrysanthemum WRKY gene *DgWRKY5* enhances tolerance to salt stress in transgenic chrysanthemum. Sci Rep. 2017;7(1):4799.
37. Nuruzzaman M, Sharoni AM, Kikuchi S. Roles of NAC transcription factors in the regulation of biotic and abiotic stress responses in plants. Front Microbiol. 2013;4:248.
38. Nie S, Wang D. AP2/ERF transcription factors for tolerance to both biotic and abiotic stress factors in plants. Trop Plant Biol. 2023;16(3):105–12.
39. Li J, Zhou H, Xiong C, et al. Genome-wide analysis R2R3-MYB transcription factors in Xanthoceras sorbifolium Bunge and functional analysis of XsMYB30 in drought and salt stresses tolerance. Ind Crops Prod. 2022;178:114597.
40. Liu H, Tang X, Zhang N, et al. Role of bZIP transcription factors in plant salt stress. Int J Mol Sci. 2023;24(9):7893.
41. Banerjee A, Roychoudhury A. Abscisic-acid-dependent basic leucine zipper (bZIP) transcription factors in plant abiotic stress. Protoplasma. 2017;254:3–16.
42. Agarwal PK, Agarwal P, Reddy MK, et al. Role of DREB transcription factors in abiotic and biotic stress tolerance in plants. Plant Cell Rep. 2006;25:1263–74.
43. Wu A, Allu AD, Garapati P, et al. JUNGBRUNNEN1, a reactive oxygen species–responsive NAC transcription factor, regulates longevity in Arabidopsis. Plant Cell. 2012;24(2):482–506.
44. Ellis JG, Tokuhisa JG, Llewellyn DJ, et al. Does the ocs-element occur as a functional component of the promoters of plant genes? Plant J. 1993;4(3):433–43.
45. Koevoets IT, Venema JH, Elzenga JTM, et al. Roots withstanding their environment: exploiting root system architecture responses to abiotic stress to improve crop tolerance. Front Plant Sci. 2016;7:1335.
46. Zhu JK. Plant salt stress. Encycl Life Sci. 2007;2:1–7.
47. Zhu JK. Abiotic stress signaling and responses in plants. Cell. 2016;167(2):313–24.
48. Yang HB, Yu YC, Wang Y, et al. Distribution and re-transportation of sodium in three Malus species with different salt tolerance. Plant Physiol Biochem. 2019;136:162–8.
49. Guo J, Lu X, Tao Y, et al. Comparative ionomics and metabolic responses and adaptive strategies of cotton to salt and alkali stress. Front Plant Sci. 2022;13:871387.
50. Li H, Tang X, Yang X, et al. Comprehensive transcriptome and metabolome profiling reveal metabolic mechanisms of *Nitraria sibirica* Pall. to salt stress. Sci Rep. 2021;11(1):12878.
51. Zhang Q, Zheng G, Wang Q, et al. Molecular mechanisms of flavonoid accumulation in germinating common bean (*Phaseolus vulgaris*) under salt stress. Front Nutr. 2022;9:928805.
52. Sarker U, Oba S. Salinity stress enhances color parameters, bioactive leaf pigments, vitamins, polyphenols, flavonoids and antioxidant activity in selected *Amaranthus* leafy vegetables. J Sci Food Agric. 2019;99(5):2275–84.
53. Ben Abdallah S, Aung B, Amyot L, et al. Salt stress (NaCl) affects plant growth and branch pathways of carotenoid and flavonoid biosyntheses in *Solanum nigrum*. Acta Physiol Plant. 2016;38:1–13.
54. Liu L, Wang B, Liu D, et al. Transcriptomic and metabolomic analyses reveal mechanisms of adaptation to salinity in which carbon and nitrogen metabolism is altered in sugar beet roots. BMC Plant Biol. 2020;20:1–21.
55. Liu CW, Chang TS, Hsu YK, et al. Comparative proteomic analysis of early salt stress responsive proteins in roots and leaves of rice. Proteomics. 2014;14(15):1759–75.
56. Jia C, Guo B, Wang B, et al. Integrated metabolomic and transcriptomic analysis reveals the role of phenylpropanoid biosynthesis pathway in tomato roots during salt stress. Front Plant Sci. 2022;13:1023696.
57. Zhang L, Zhang Z, Fang S, et al. Integrative analysis of metabolome and transcriptome reveals molecular regulatory mechanism of flavonoid biosynthesis in *Cyclocarya paliurus* under salt stress. Ind Crops Prod. 2021;170:113823.
58. Hussein MM, Faham SY, Alva AK. Role of foliar application of nicotinic acid and tryptophan on onion plants response to salinity stress. J Agric Sci. 2014;6(8):41.
59. Khare S, Singh NB, Singh A, et al. Plant secondary metabolites synthesis and their regulations under biotic and abiotic constraints. J Plant Biol. 2020;63:203–16.

60. Wu Y, Zhu K, Wang C, et al. Comparative metabolome and transcriptome analyses reveal molecular mechanisms involved in the responses of two *Carex rigescens* varieties to salt stress. Plants. 2024;13(21):2984.
61. Yuan G, Sun D, An G, et al. Transcriptomic and metabolomic analysis of the effects of exogenous trehalose on salt tolerance in watermelon (*Citrullus lanatus*). Cells. 2022;11(15):2338.
62. Chinnusamy V, Jagendorf A, Zhu JK. Understanding and improving salt tolerance in plants. Crop Sci. 2005;45(2):437–48.
63. Zhang D, Hu Y, Tang L, et al. ABCG transporters in the adaptation of rice to salt stresses. Int J Mol Sci. 2024;25(19):10724.
64. Shi H, Ye T, Chen F, et al. Manipulation of arginase expression modulates abiotic stress tolerance in Arabidopsis: effect on arginine metabolism and ROS accumulation. J Exp Bot. 2013;64(5):1367–79.
65. Ahmad I, Zhu G, Zhou G, et al. Pivotal role of phytohormones and their responsive genes in plant growth and their signaling and transduction pathway under salt stress in cotton. Int J Mol Sci. 2022;23(13):7339.
66. Wang GL, Ren XQ, Liu JX, et al. Transcript profiling reveals an important role of cell wall remodeling and hormone signaling under salt stress in garlic. Plant Physiol Biochem. 2019;135:87–98.
67. Xiong Y, Yan H, Liang H, et al. RNA-Seq analysis of *Clerodendrum inerme* (L.) roots in response to salt stress. BMC Genomics. 2019;20:1–18.
68. Zhu Y, Wang Q, Gao Z, et al. Analysis of phytohormone signal transduction in sophora alopecuroides under salt stress. Int J Mol Sci. 2021;22(14):7313.
69. Liu Q, Li P, Cheng S, et al. Protoplast dissociation and transcriptome analysis provides insights to salt stress response in cotton. Int J Mol Sci. 2022;23(5):2845.
70. Chen L, Meng Y, Bai Y, et al. Starch and sucrose metabolism and plant hormone signaling pathways play crucial roles in aquilegia salt stress adaption. Int J Mol Sci. 2023;24(4):3948.
71. Chen Y, Jiang Y, Chen Y, et al. Uncovering candidate genes responsive to salt stress in *Salix matsudana* (Koidz) by transcriptomic analysis. PloS one. 2020;15(8):e0236129.
72. Liu Y, Ji D, Turgeon R, et al. Physiological and proteomic responses of mulberry trees (*Morus alba*. L.) to combined salt and drought stress. Int J Mol Sci. 2019;20(10):2486.
73. Pi E, Zhu C, Fan W, et al. Quantitative phosphoproteomic and metabolomic analyses reveal GmMYB173 optimizes flavonoid metabolism in soybean under salt stress. Mol Cell Proteomics. 2018;17(6):1209–24.
74. Liu L, Zhang P, Feng G, et al. Salt priming induces low-temperature tolerance in sugar beet via xanthine metabolism. Plant Physiol Biochem. 2023;201:107810.
75. Li S, Chang L, Sun R, et al. Combined transcriptomic and metabolomic analysis reveals a role for adenosine triphosphate-binding cassette transporters and cell wall remodeling in response to salt stress in strawberry. Front Plant Sci. 2022;13:996765.
76. Sui D, Wang B, El-Kassaby YA, et al. Integration of physiological, transcriptomic, and metabolomic analyses reveal molecular mechanisms of salt stress in *Maclura tricuspidata*. Plants (Basel). 2024;13(3):397.
77. Nakabayashi R, Saito K. Integrated metabolomics for abiotic stress responses in plants. Curr Opin Plant Biol. 2015;24:10–6.
78. Wang Y, Mostafa S, Zeng W, et al. Function and mechanism of jasmonic acid in plant responses to abiotic and biotic stresses. Int J Mol Sci. 2021;22(16):8568.
79. Maeda H, Dudareva N. The shikimate pathway and aromatic amino acid biosynthesis in plants. Annu Rev Plant Biol. 2012;63(1):73–105.
80. Fernie AR, Martinoia E. Malate. Jack of all trades or master of a few? Phytochemistry. 2009;70(7):828–32.
81. Dabravolski SA, Isayenkov SV. The role of histidine kinase signalling in response to salt stress. Plant Soil. 2023:147–61.
82. Obata T, Fernie AR. The use of metabolomics to dissect plant responses to abiotic stresses. Cell Mol Life Sci. 2012;69(19):3225–43.
83. Sharma A, Shahzad B, Rehman A, et al. Response of phenylpropanoid pathway and the role of polyphenols in plants under abiotic stress. Molecules. 2019;24(13):2452.
84. Corpas FJ, Gupta DK, Palma JM. Tryptophan: a precursor of signaling molecules in higher plants. Horm Plant Response. 2021;2:273–89.
85. Majumdar R, Barchi B, Turlapati SA, et al. Glutamate, ornithine, arginine, proline, and polyamine metabolic interactions: the pathway is regulated at the post-transcriptional level. Front Plant Sci. 2016;7:78.
86. Joshi V, Jander G. Arabidopsis methionine γ-lyase is regulated according to isoleucine biosynthesis needs but plays a subordinate role to threonine deaminase. Plant Physiol. 2009;151(1):367–78.
87. Yang Q, Zhao D, Liu Q. Connections between amino acid metabolisms in plants: lysine as an example. Front Plant Sci. 2020;11:928.
88. Ji Y, Li Q, Liu G, et al. Roles of cytosolic glutamine synthetases in Arabidopsis development and stress responses. Plant Cell Physiol. 2019;60(3):657–71.
89. Gaufichon L, Rothstein SJ, Suzuki A. Asparagine metabolic pathways in Arabidopsis. Plant Cell Physiol. 2016;57(4):675–89.
90. Yang L, Han H, Liu M, et al. Overexpression of the Arabidopsis photorespiratory pathway gene, serine: glyoxylate aminotransferase (AtAGT1), leads to salt stress tolerance in transgenic duckweed (*Lemna minor*). Plant Cell Tiss Organ Cult. 2013;113:407–16.
91. Duan Y, Li F, Li Y, et al. The role of leucine and its metabolites in protein and energy metabolism. Amino Acids. 2016;48(1):41–51.
92. Huang T, Jander G. Abscisic acid-regulated protein degradation causes osmotic stress-induced accumulation of branched-chain amino acids in Arabidopsis thaliana. Planta. 2017;246:737–47.
93. Wu Y, Zhu K, Wang C, et al. Comparative Metabolome and Transcriptome Analyses Reveal Molecular Mechanisms Involved in the Responses of Two *Carex rigescens* Varieties to Salt Stress. Plants (Basel). 2024;13(21):2984.
94. Hildebrandt TM. Synthesis versus degradation: directions of amino acid metabolism during Arabidopsis abiotic stress response. Plant Mol Biol. 2018;98(1-2):121–35.

Publisher's Note